NASA TECHNICAL NOTE

NASA TN D-2224

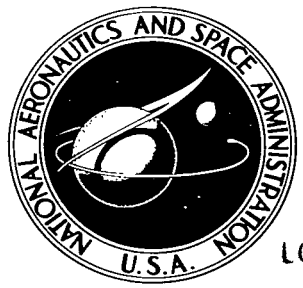

NASA TN D-2224

A STUDY OF OXIDATION KINETICS OF NICKEL METAL IN FLOWING AIR AND OXYGEN-NITROGEN MIXTURES

by D. J. Progar and B. W. Lewis

Langley Research Center

Langley Station, Hampton, Va.

NATIONAL AERONAUTICS AND SPACE ADMINISTRATION • WASHINGTON, D. C. • DECEMBER 1964

A STUDY OF OXIDATION KINETICS OF NICKEL METAL IN FLOWING AIR AND OXYGEN-NITROGEN MIXTURES

By D. J. Progar and B. W. Lewis

Langley Research Center
Langley Station, Hampton, Va.

NATIONAL AERONAUTICS AND SPACE ADMINISTRATION

For sale by the Office of Technical Services, Department of Commerce,
Washington, D.C. 20230 -- Price $1.50

A STUDY OF OXIDATION KINETICS OF NICKEL METAL IN FLOWING AIR AND OXYGEN-NITROGEN MIXTURES

By D. J. Progar and B. W. Lewis
Langley Research Center

SUMMARY

A study was made of the oxidation kinetics of nickel metal sheet in flowing air and in oxygen-nitrogen mixtures of varying composition. The study covered the temperatures 1500° F, 1750° F, 2000° F, 2250° F, and 2500° F and covered flow conditions of natural convection and 0.065, 0.130, 0.205, and 0.280 standard ft^3/min for the air study and 0.130 and 0.280 standard ft^3/min for the oxygen-nitrogen mixture study. The oxygen partial pressures of the gas mixtures used were 380, 76, 38, and 7.6 mm mercury. A thermogravimetric technique was used to obtain the rate data. The data showed the reaction in the thick-film region to follow a parabolic-rate-law characteristic of a mechanism in which diffusion through a crystalline solid is rate controlling. The reaction-rate constants and energy of activation obtained agree reasonably well with most other experiments in the literature in which there was no forced flow of gas. This study showed no effect of flow on the reaction-rate constants for air but did show a slight decrease in reaction-rate constants for an approximately doubled flow rate for the oxygen-nitrogen gas mixtures. Examinations of the nickel and the oxide by X-ray diffraction and optical microscopy were performed.

INTRODUCTION

The oxidation of metals at temperatures below their melting point is often a limiting factor in their use. Whereas the metal itself may retain acceptable physical properties at high temperatures, its oxide generally has poor properties and thus knowledge of the rate at which oxidation occurs for a range of temperatures and conditions of exposure to oxygen is important in many applications. Not only is the rate itself of importance but knowledge of the mechanism and effects of various other factors on the rate may determine the metal's usefulness. Studies of the reaction kinetics of metal oxidation yield not only quantitative reaction rates but reveal information as to the mechanism of the reaction. By knowing a mechanism, it is sometimes possible to devise a method of changing the reaction rate by providing barriers to access of the reacting species or by providing alternate rate-determining paths. Generally, kinetics studies are performed over as great a range of variables as is possible with good control. In the present case the authors were interested in studying the oxidation kinetics of nickel metal in a flowing gas stream while developing a

general technique for such studies. Nickel has been studied by a number of investigators (refs. 1 to 6) whose works present a fairly consistent picture of the oxidation kinetics but did not include any studies of the effects of flowing gas. These references show that the nickel oxidation reaction follows a parabolic rate "law" and has an activation energy E_a of about 44 kcal/mole in the range of 1000° F to 2500° F with some exceptions and for several different partial pressures of oxygen. Differences have been noted in the parabolic reaction-rate constants k_p and the E_a for specimens of different purity and for different impurities when compared at a given temperature. A generally accepted mechanism for the thick-film oxidation (as distinguished from the initial thin film region) has been developed by others and is based on the theory of Wagner (ref. 5) in which the reaction rate is believed to be controlled by the diffusion of Ni^{2+} cations through the nickel oxide NiO from the metal-oxide interface to the oxide-gas interface. This mechanism is supported by experiments of the conductivity of NiO both pure and when doped with certain impurities and also by studies of the thermoelectric effects in NiO. According to the Wagner theory, the reaction-rate constants for nickel oxidation should be dependent on the one-sixth root of the oxygen partial pressure $\left(p_{O_2}{}^{1/6}\right)$ and some experiments have been reported which showed such a dependency when the p_{O_2} was less than 100 mm mercury. (See ref. 7.)

If this parabolic mechanism is correct, one would not expect that the flow of oxidizing gas over the oxide surface would have any effect on the rate of reaction; however, a few investigations of the effect of flowing gases on other parabolic metal oxidation reactions have shown effects, sensitive to temperature ranges, which varied from significant changes in rate to none at all. (See ref. 5, pp. 77-78.) No specific explanation of these effects has been found. It has been suggested (ref. 5) that flowing gases at various rates have an influence on the oxide-film formation and result in imperfections or defects not found in stagnant systems or for all ranges of flow and temperature.

In the present study there were two objectives: (1) to develop and check out the technique of measurement of metal oxidation rates using a metal nickel for which there was a relatively large amount of reliable kinetic data and for which an accepted mechanism was available; and (2) to determine whether the flow of gases over the specimens influenced the rates of oxidation.

The study was performed essentially in two phases. The first was a series of kinetic runs using air as the oxidizing gas at the temperatures 1500° F, 1750° F, 2000° F, 2250° F, and 2500° F and four volumetric air flow rates each, and having linear velocities spread between 0.6 and 3.6 ft/sec as well as a convection case with no forced flow. Parabolic reaction-rate constants k_p were obtained for each of these runs and the energy of activation E_a was obtained by use of an Arrhenius plot of the variation of $\log k_p$ with the reciprocal of the absolute temperature $1/T$. All specimens were cut from the same sheet of nickel and thus reasonable uniformity of specimen composition was assumed. The second phase was a series of runs in which the partial pressure of O_2 was varied

in O_2-N_2 gas mixtures. Gas mixtures having p_{O_2} of 380, 76, 38, and 7.6 mm Hg were metered at flow rates of 1.23 ft/sec to 1.76 ft/sec, and 2.31 ft/sec to 3.64 ft/sec over the Ni specimens at the temperatures 1750° F, 2000° F, 2250° F, and 2500° F. The two phases are treated separately to avoid confusion since there were differences in procedure and emphasis.

Besides the kinetic runs, a study was made of the physical nature of the NiO scales by use of X-ray diffraction techniques and photomicrography to determine relative crystal size and orientation effects if any.

SYMBOLS

a	proportionality constant $\left(\text{in equation } k = a\left(p_{O_2}\right)^{1/n}\right)$
A	empirical constant
E_a	activation energy, kcal $mole^{-1}$
I	intensity of X-ray diffraction peak
I_1	highest intensity X-ray diffraction peak
k	specific reaction-rate constant
k_p	parabolic reaction-rate constant, $g^2cm^{-4}sec^{-1}$
$\bar{k}_p$	average k_p of four flow rates and convective condition for a particular temperature, $g^2cm^{-4}sec^{-1}$
Δm	weight change per unit specimen area at any time, gcm^{-2}
1/n	exponent of p_{O_2} in expression relating k_p to p_{O_2}
p_{O_2}	partial pressure of oxygen, mm Hg
R	universal gas constant, 1.987 cal $mole^{-1}$ $(°K)^{-1}$
T	absolute temperature, °K
t	time
W_F	weight of oxidized specimen after removed from furnace, g
W_L	last weight of specimen recorded before removed from furnace, g

APPARATUS AND PROCEDURE

For this study of the oxidation kinetics of nickel a method of measuring the weight change as a function of time was selected. (See ref. 5.) For this technique, the nickel specimen was suspended by an inert (platinum) wire from the arm of an analytical chainomatic balance into the oxidation furnace. This technique was chosen for this investigation because it permitted a semicontinuous measurement of the weight change as a function of time while the specimen was in the oxidizing atmosphere. A schematic drawing of the thermobalance and associated components used in this investigation is given in figure 1. Two different gas inlet trains are shown: one is for the runs using air and the other, for oxygen-nitrogen mixtures.

For the air-oxidation studies, air from a high-pressure line was passed through a purification system composed of separate glass containers filled with a sodium hydrate asbestos absorbent and silica gel (a dehydrated silicon dioxide) for the removal of carbon dioxide and water vapor, respectively. For the oxygen-nitrogen gas mixtures, oxygen of 99.5-percent purity obtained in cylinders was delivered through a diaphragm regulator and a needle valve and passed through a purification train such as was described for air. The oxygen flow rate was controlled by a calibrated glass flow meter with the inlet pressure measured by a Bourdon gauge and regulated by a needle valve. Nitrogen of 99-percent purity with hydrogen (maximum 1 percent, average analysis 0.5 percent) as its principal impurity followed a duplicate system. The two gases were mixed at various flow rates such that the mixture had oxygen partial pressures of 380, 76, 38, or 7.6 mm Hg as required for a particular oxidation experiment. Slight deviations in the pressure, either from the air-pressure line for the air-flow system or the oxygen or nitrogen pressure regulation for the oxygen-nitrogen system, were minimized by connecting a surge tank (an equalizing reservoir) to the system. The air was metered by a flow meter following the surge tank. From this point on, the two systems were the same. The gas passed through a wire-wound combustion tube furnace with small-diameter ceramic tubing filling the interior of the fused alumina tube providing a greater surface area for heat transfer to the gas. This gas preheat furnace was operated at its maximum rated temperature of 1800° F controlled by an autotransformer. The temperature of the preheater was measured by a chromel-alumel thermocouple located half the length of the furnace tube and touching the tube wall. Zirconia pebbles approximately 3/8 inch in diameter filled a metal elbow connecting tube between the preheat furnace and the oxidation tube to improve flow uniformity in the oxidation tube. The oxidation furnace used was a commercial combustion tube furnace which was placed so that the tube was in a vertical position. Because of the long time required to obtain the desired temperatures and the insensitive temperature control of the standard power supply furnished with the furnace, it was advantageous to use a different power supply to obtain shorter heat-up time and closer temperature regulation. A power supply consisting of two 20-ampere 120-volt autotransformers connected in parallel was therefore used. The mullite oxidation tube, $1\frac{1}{2}$ inches outside diameter and $1\frac{3}{16}$ inches inside diameter by 22 inches long was heated by three resistance-matched silicon carbide rods. A shielded thermocouple connected to a temperature-indicating meter was located between the resistance rods and

adjacent to the mullite tube. Placed above the furnace was a water-cooled shield to prevent heat being given off by the furnace from affecting the balance. Above this shield was a small cone-shaped water-cooled shield to prevent air currents from deflecting the specimen suspension wire. A modified analytical chainomatic balance with a sensitivity of 0.1 milligram was used to determine the weight measurements during a kinetic run. The balance was modified by grinding a 1/4-inch-diameter hole in the glass base of the balance under the left arm of the beam. The left pan was removed and a heat-resistant glass tube with platinum wire in the shape of a hook sealed in both ends of the tube was substituted. The glass tube extended below the base of the balance from which a nickel specimen was suspended on No. 30 gage (B & S) platinum wire. In order to be sure that the experimental conditions were controllable and comparable for the various runs and to minimize temperature and weighing errors, the system was thoroughly profiled and calibrated under all conditions of flow and temperature to be used. (See appendix for details.)

As a result of the temperature survey of the furnace and system, it was known that the temperature of the gas flowing past the specimen was lower than the temperature of the specimen and the difference in these temperatures depended on the flow rate of gas. This nonequilibrium condition made it necessary to define the reaction temperature for this study in a manner in which it was considered to be least likely to produce errors or inconsistencies. The reaction temperature was therefore defined to be the nickel-specimen temperature, a condition which could most readily be controlled during a run. Table I gives the linear flow rates for each condition of temperature and volume flow rate calculated as an average over the center part of the tube. It was experimentally determined that the temperature of the specimen during a run could routinely be controlled to within $\pm 15^{\circ}$ F of the desired value and usually was better than $\pm 10^{\circ}$ F. See the appendix and the two typical specimen temperature-time plots shown in figure 2.

Nickel Specimens

The 0.005-inch-thick nickel sheet used in the investigation was of a commercial grade: 99.5 ± 0.3 percent pure determined by electrolytic deposition and with the impurities Zn, Fe, Co, Ag, Se, and Mn being indicated by X-ray spectrochemical analysis. Several shapes and sizes of specimens were tested for the least temperature gradient across the specimen surface. It was found that a specimen 2 centimeters by 2 centimeters gave the best results. This specimen size was used throughout the experiments. Specimens were cold sheared to size and a 0.109-centimeter-diameter (0.0429-inch) hole was punched close to one edge for hanging. They were measured with a micrometer caliper to the nearest thousandth of an inch, cleaned in ethyl alcohol and acetone, and then stored in a dessicator until needed. At this time they were cleaned again in the same manner, weighed on an analytical chainomatic balance having a sensitivity of 0.1 milligram, and then used for the experiment. The specimens weighed between 0.4730 and 0.4229 gram and had a surface area between 8.45 and 7.92 square centimeters. The area of the 0.109-centimeter hole and the area of the edges of the specimen were taken into consideration when specimen surface area was determined.

Experimental Procedure

For the air oxidation studies, the air was adjusted to the desired flow rate, except for the natural convection condition where the air line was disconnected before the purification train. For the oxygen-nitrogen mixture studies, the two gases were mixed in such a way that for the total flow rates used, 0.130 standard ft^3/min and 0.280 standard ft^3/min, the gas had the oxygen partial pressure desired. This condition was obtained by adjusting the separate flow rates for oxygen and nitrogen on their respective flow meters and mixing them before they entered the preheater. The preheater furnace was heated to 1800° F with the gas flowing. The preheating raised the temperature of the gas leaving the preheater furnace to approximately $700^\circ \pm 20^\circ$ F for the convective flow. The temperature of the oxidation furnace was raised to the desired temperature for the gas flow condition and specimen temperature desired. These values were predetermined from a calibration curve of the nominal furnace temperature plotted against specimen temperature for the various flow rates used.

The calibration curve was obtained and checked by spot welding a thermocouple to a nickel specimen and measuring the electromotive force on a manual balance precision potentiometer for a particular depth of the specimen in the oxidizing tube. Typical calibration curves are shown in figure 3. The specimen was cleaned as described earlier, weighed on a separate analytical chainomatic balance, and the weight recorded. This weight was the original weight of the specimen before oxidation. This specimen was then hung on the platinum wire suspended below the balance. When the furnaces had reached thermal equilibrium, the specimen was dropped into the hot zone of the oxidation furnace and a stop watch was started simultaneously. Weight measurements were recorded periodically (usually at 5-minute intervals) for runs lasting between 60 and 120 minutes. The balance was adjusted to the equilibrium position manually as necessary to make the readings.

After the last weight W_L was recorded, the specimen was immediately removed from the furnace, air cooled quickly to room temperature, and weighed on the separate analytical chainomatic balance to give the final weight W_F. Since it was difficult, if not impossible, to make an accurate weighing at zero time because of the finite time required for temperature (about 30 seconds) and balance equilibrium after dropping the specimen into the furnace, a special procedure was adopted. Drag was determined as $W_F - W_L$ and all readings were corrected accordingly. Since the desired quantity was the weight change per unit area, the specimen weight change for each time interval was divided by the surface area of the specimen. The sum of these weight changes per unit area for each period was designated as a Δm quantity. Thus, Δm is a measure of the extent of oxidation which had taken place after a given period of time under the conditions of the run.

X-Ray Examination Procedure

Specimens of unoxidized nickel, oxidized nickel specimens with the outer thick oxide removed by successive flexing and leaving a light green or gray-green

oxide exposed, and oxidized nickel specimens were examined by an X-ray diffractometer using Cu K_α-radiation. These specimens, except for the pure (99.5 ± 3 percent) nickel were from kinetic oxidation runs at an oxygen partial pressure of 76 mm Hg, gas flow rates of 0.130 and 0.280 standard ft^3/min, and temperatures of about 1750° F, 2000° F, 2250° F, and 2500° F. All the oxide coatings were adherent. The oxide on 1750° F specimen would not crack off upon repeated bending; therefore, no X-ray examination of the substrate oxide could be made. Comparison of X-ray charts were made by taking the highest intensity nickel oxide peak to be 100, that is I_1, and taking a ratio of the other peaks I to it, that is, I/I_1.

RESULTS AND DISCUSSION

The kinetic measurements in both phases of this study yielded oxidation rates which followed a parabolic relationship, that is,

$$(\Delta m)^2 = k_p t$$

where Δm is the weight change per unit area of the specimen at any time t and k_p is the parabolic rate constant. The k_p values were obtained for a run by taking the slope of the least-squares straight-line plot of $(\Delta m)^2$ against t. Figures 4 to 8 show typical data plots of this type for a variety of air oxidation run conditions. The linearity of these plots indicates that a parabolic rate is being followed. It can be seen that some runs gave data plots which had two straight-line regions of different slope, a shorter region at the beginning of the run with a greater slope and a longer region of lesser slope after the run had been in progress for a short time. Other runs are seen to give plots of a single straight line. These differences are interpreted as follows: the plots having two slopes show behavior associated with two mechanisms, an initial thin-film (tarnish) mechanism and a final thick-film (scale) mechanism both of which are parabolic (solid diffusion controlled). An uncertainty is also present for the initial part of the slower oxidation rate runs since the weight changes are of about the same order of magnitude as the balance sensitivity. The single slope curves are obtained for runs in which the oxidation rate is high enough so that the thick film is formed during the first time interval. Since there was this type of variation in mechanisms within the experimental ranges of this study, only the k_p values for the thick film (scale), following the Wagner mechanism, are tabulated and compared. The values of k_p obtained for the air oxidation runs at temperatures 1500° F, 1750° F, 2000° F, 2250° F, and 2500° F at each of five flow rates; convection, 0.065, 0.130, 0.205, and 0.280 standard ft^3/min are given in table II. These values were obtained by least-squares calculations of the best straight line through the data points judged to comprise the thick-film part of each run. A $\bar{k}_p$ value is tabulated for each temperature which is the average k_p value for the five flow conditions. Values of k_p in table II are all for single runs except the 0.065 and 0.205 standard ft^3/min runs at 1500° F of which there are two runs each.

Table III gives the k_p values for the O_2-N_2 oxidation runs for temperatures of 1750° F, 2000° F, 2250° F, and 2500° F at each of the flow rates of 0.130 and 0.280 standard ft^3/min for each of the O_2-N_2 mixtures having p_{O_2} of 380, 76, 38, 7.6 mm Hg and figures 9 to 12 show typical plots of $(\Delta m)^2$ against t for this type of run. Again the plots with two slopes and one slope are interpreted as before. Since the actual data obtained for the O_2-N_2 runs were obtained at temperatures somewhat different than the nominal temperatures of 1750° F, 2000° F, 2250° F, and 2500° F, the values for these round-number temperatures were obtained from Arrhenius plots of the actual run data. The values of k_p in table III are thus given for the round-number temperatures in order to make comparisons of the effect of flow rate and composition at the various test temperatures. The k_p values in table III are the average result of two or more runs for each condition.

The energy of activation E_a is obtained by use of the Arrhenius equation:

$$k = Ae^{-E_a/RT}$$

where k is the reaction-rate constant, A is an empirical constant, e is the base of natural logarithms, R is the universal gas constant, and T is the absolute temperature. This equation is an empirical one which expresses the effect of temperature on the rates of most kinetic processes. The value E_a is obtained from the slope of a plot of $\log k_p$ against $1/T$, the slope being equal to $-E_a/2.303R$. Figure 13 is the Arrhenius plot for the air oxidation data of this study and the value of E_a obtained from this plot is 41.3 kcal/mole. Figures 14(a) and 14(b) show Arrhenius plots of the data of the O_2-N_2 oxidation study where E_a values vary from 42.3 to 45.6 kcal/mole for the runs at 0.130 standard ft^3/min and from 43.3 to 46.5 kcal/mole for the runs at 0.280 standard ft^3/min. The E_a values for this phase of the study show a trend of increasing E_a with p_{O_2} for each of the flows.

Figures 15 show plots of k_p against flow rate in standard ft^3/min for the air oxidation runs for each of the temperatures of the study. These figures show that there is no significant effect of flow rate of air in the range studied since the values of k_p are randomly distributed about an average value for each temperature. An analysis of the repeatability of k_p determinations by several runs for various conditions showed the variation of the data taken was within a range of 6.5 percent at 1750° F to 4.7 percent at 2500° F. Thus, the scatter in the data was considered to be due to random experimental errors. The probable variation of k_p for a 15° F error in average temperature (experimentally determined temperature control limit) of the specimen during a run was calculated by use of the Arrhenius equation after having obtained the values for the constants A and E_a from the $\bar{k}_p$ values for the temperatures of the air oxidation studies. The difference in k_p which would result from a 15° F temperature error amounted to 14.8 percent at 1500° F and decreased regularly with

increasing temperature to 6.6 percent at 2500° F. By consulting figures 15(a) to 15(e), it may be shown that the deviations of k_p at a given temperature and for all flow rates are less than the possible error because of the lack of precise temperature control. The scatter may, however, be due mainly to the temperature control factor.

The specimens were cut from a single sheet of nickel and were cleaned and prepared for test by the same procedure each time. The literature has shown that such factors as surface roughness, primary oxide film, percent purity, and presence of certain impurities may have varying effects on the oxidation rate of nickel. When the results of this air oxidation study are compared with those in the literature which were for essentially nonflowing systems, these factors need to be kept in mind and also that the partial pressure of O_2 has a small effect. One way of comparing results is to examine the Arrhenius plots and the E_a values for the various studies as may be done by use of figure 16. The data shown in figure 16 do not include all the studies of nickel oxidation in the literature since the specific data required to make the plots were not available in many cases. However, E_a values were given in most cases and most were in the 40 to 50 kcal/mole range. The differences in the kinetics between the various studies probably reflect differences in percent purity, impurity species, O_2 partial pressure, or experimental methods including specimen surface condition. Variations of as much as tenfold in the k_p values have been shown in reference 5 (from the work of Von Goldbeck) to result from varying the amounts and/or kinds of impurities and these variations seem to be about the same as those shown in the investigations compared in figure 16. According to the theory describing cationic diffusion mechanisms, the presence of certain types of cationic impurities in the oxide lattice will affect significantly the rate of diffusion of the Ni^{2+} cations through the NiO lattice. Thus, the air oxidation data obtained in this investigation are considered to agree reasonably well with others in the literature. The generally accepted thick-film mechanism for oxidation of nickel is supported by this study and no effect of flow was observed in the air oxidation rates measured.

In the second phase of these oxidation studies, the effects of O_2 partial pressure and flow were investigated for several temperatures. The k_p values have been presented in table III and E_a values are given in figure 14 as has previously been mentioned. According to the theory of Wagner, the general relationship between reaction-rate constant and p_{O_2} for a reaction of this type is

$$k = a\left(p_{O_2}\right)^{1/n}$$

where a is a proportionality constant and n depends on the stoichiometry of the rate-determining reaction process. A value of 6 for n has been derived theoretically for thick-film nickel oxidation. In order to test this theoretical value of n with the experimental data of this study, the variation of the log of k_p with log p_{O_2} was plotted and the slope of the straight-line portion

of the curve was obtained to give $1/n$. Figures 17(a) to 17(h) are the plots of the variation of $\log k_p$ with $\log p_{O_2}$ and table IV gives the values of n derived from these plots. It may be seen from these plots that the linear relationship predicted by the equation is followed by the three points for the p_{O_2} of 7.6, 38, and 76 mm Hg and the tendency is for k_p to become less sensitive to p_{O_2} somewhere between 76 and 380 mm Hg. Reference 1 indicates that others have placed the threshold of sensitivity to p_{O_2} below the vicinity of 76 to 100 mm Hg of O_2 for high purity Ni. The values of n which were obtained in this study varied with temperature and with flow rate but averaged about 6.1. This condition seems to indicate that the mechanism assumed in arriving at the theoretical value of 6 for n is probably correct for the major diffusion process. The fact that the values of n show trends with temperature and flow could indicate varying contributions from other simultaneous modes of diffusion which were more or less dependent on temperature or surface conditions. It is certain that more than a single diffusion mechanism occurs in NiO, and impurities complicate the diffusion and the overall oxidation process.

It has been noted (ref. 5, p. 78) that small amounts of inert gases may affect the adsorption processes of O_2 and thus the oxidation rates. The data obtained in this study may indicate that some such effects were encountered if the O_2-N_2 runs and the air runs are compared. When the air runs $\left(p_{O_2} = 159 \text{ mm Hg}\right)$ were plotted with the O_2-N_2 runs in plots of k_p against p_{O_2}, the air points varied randomly with respect to the straight-line portions of the O_2-N_2 points for the different temperatures. This condition might be due to some variation in gas impurity effects or might also be due to a more refined technique which had been developed by the time the O_2-N_2 runs were made. Thus for these reasons the air data were not included in the plots of figure 17.

In connection with the gas impurity effects, consideration of the effect of the H_2 impurity present in the N_2 used in this study is in order. As was stated previously, the N_2 used contained an average of 0.5 percent H_2 with a maximum of 1 percent. In O_2-N_2 mixtures of relatively high O_2 content, the H_2 impurity would be negligible as a reactant, but at the lowest O_2 content mixtures the H_2 would be of about the same order of magnitude as the O_2. That the H_2 may react with NiO to reduce it back to the metal is a possibility. However, a consideration of the free-energy changes of the possible reactions, that is, oxidation of Ni by O_2 and reduction of the product NiO by H_2, indicates that the oxidation reaction is clearly favored thermodynamically over the temperature range of this study. That the presence of H_2 in the metal may affect the nucleation and rate of growth of NiO scale has been shown by studies of the oxidation of Ni single crystals by Lawless, Young, and Gwathmey (ref. 8). They also obtained data showing different rates of oxidation for different crystal faces of Ni. Thus, it is believed that the oxidation rates for the O_2-N_2 runs may have been affected by the presence of H_2 compared with the air runs but only as a consequence of nucleation effects rather than of the reduction reaction.

In studying the data of table III, it will be noted that definite trends are apparent. First, k_p varies with p_{O_2} as just discussed. Next, whereas there was no tendency for the air oxidation runs to show a systematic variation with air flow rate, the O_2-N_2 runs showed a small but consistent decrease in k_p values for an approximately twofold increase in gas flow rate. The reason for such an effect is not known; however, as pointed out earlier, variations in rate have been observed for parabolic-type oxidations when flow rates were varied and in some cases maxima have been obtained. (See ref. 5.) It would appear that the most plausible explanation of these types of observed effects is that the flow of gases over the surface has an influence on the morphology and orientation of the oxide layer (ref. 5) which affects the diffusion rates of ions in the oxide and hence the oxidation rate.

There was a noticeable difference in the appearance of the oxidized specimens with change in temperature and/or oxidation rate. Table V gives information on the colors of the oxide surface and the subsurface oxide when the outer scale was removed by flaking off with bending of the specimens for all of the O_2-N_2 runs. The color variations appeared to be more closely related to temperature than to flow or p_{O_2}. The lower temperatures (1750° F and 2000° F) gave thin smooth coatings with a greenish cast. The 2250° F specimens had a gray smooth coating and the 2500° F specimens had a dark gray somewhat shiny but rough surface. In order to determine whether there were any detectable crystallographic or orientation differences in the variously appearing oxides, some X-ray diffraction studies were made of the unoxidized nickel and for the outer oxide surface and the subsurface oxide for the runs with the p_{O_2} of 76 mm Hg. The results of these studies of the oxide are shown in figures 18 to 21. These figures are plots of the variation of peak height (intensity) ratios I/I_1 of the various lattice planes of NiO (designated by Miller indices) normalized to the most intense I_1 as 100 with temperature at which the specimen had been run. In figures 18 and 19 when runs at 0.130 standard ft^3/min flow are compared, the peak for the 111 plane of the outer oxide for the 2500° F specimen was most intense and in figures 20 and 21, when runs at 0.280 standard ft^3/min flow are compared, the peak for the 200 plane of the outer oxide for the 2000° F specimen was most intense. These figures indicate definite preferred orientation exists for these specimens parallel to the sheet. For a powder sample (random orientation) of NiO, the ASTM powder data file (ref. 9) gives the most intense peak as the 200 plane, the 111 plane being slightly less intense. For the outer surfaces (greenish gray to dark gray) of the specimens (figs. 18 and 20) the 200 and 111 planes appear to have about the same degree of intensity as the powder data in the lower specimen temperature range but as the temperature at which the specimen was run increased above about 2100° F, a definite preferred orientation of the 111 plane developed as relative intensities of the 200 plane dropped rapidly while the relative intensity of the 111 plane increased rapidly (fig. 18) or remained high (fig. 20). All other planes present on the outer surface were of low intensity and changed relatively little with temperature. Figures 19 and 21 show the preferred orientation for the subsurface oxide layer (light green). The 200 plane here has the highest ratio and has a maximum value at about 2250° F for both flow rates; however, the 111 plane has very low intensity ratios and thus indicates a preferred

orientation effect in that it differs from the random powder pattern. This orientation is following that of the unoxidized nickel metal surface which was determined to have a high degree of orientation in the 200 plane with very little 111 plane showing as opposed to the nickel powder pattern in which the 111 plane is most intense and the 200 plane only moderate. From these X-ray data, there is no clear evidence of preferred orientation differences which might explain the trend in the values of k_p with flow rate for the O_2-N_2 mixtures. There are, however, indications in the literature that orientation differences can definitely affect the oxidation rate by varying the diffusion rates. (See, for example, ref. 10.)

There is a possible correlation between the preferred orientation of the outer oxide surface and color as it appears that the trend from a greenish gray to a dark gray outer surface coincides with an increasing intensity from the 111 plane accompanied by the decrease in intensity from the 200 plane at the surface. Others (ref. 11) have based explanations of the color differences as being due to a variation in lattice content of oxygen ions (O^{2-}), the higher content giving the dark gray color.

Results of microscopic examinations of the oxide surfaces, both the outer surface and the subsurfaces (light green) showed in both cases that the crystal form became more regular as the temperature of the test increased and also that the average crystal size increased with test temperature.

The results of the O_2-N_2 oxidation studies showed a small but significant decrease in oxidation rate for an approximately doubled gas flow rate over a temperature and p_{O_2} range. The reason for this seemingly anomalous behavior has not been determined but it should be noted that this type of behavior has been observed by others in studies of different parabolic oxidation systems. (See ref. 5.) Some possible explanations for this behavior involve differences in adsorption rate of O_2, nucleation site formation, orientation or crystal growth all of which can affect the diffusion mechanisms and rates in the oxide layer. It appears that different types of studies are necessary to obtain specific information bearing on these possibilities.

CONCLUDING REMARKS

This study of the kinetics of nickel metal oxidation in the temperature range 1500° F to 2500° F and for flow rates from natural convection to 0.280 standard ft^3/min for air and for O_2-N_2 mixtures has shown that flow in the range tested for the air study had no measurable effect on the oxidation rate of nickel. The rate constants k_p and the energy of activation E_a determined were in reasonable agreement with other studies in the literature. The E_a value determined from the air data was 41.3 kcal/mole and for the O_2-N_2 mixtures, the E_a value ranged between 42.3 and 46.5 kcal/mole. The study of the effect of O_2 partial pressure indicated that the k_p values were

dependent on $p_{O_2}^{1/n}$ where average values of n varied from 7.14 to 5.14 for the 0.130 and 0.280 standard ft^3/min flow rates, respectively. Since the theoretical value of n for a mechanism involving the diffusion of Ni^{+2} ions in the NiO lattice is 6, the values obtained in this study would tend to indicate that this mechanism is probably responsible for most of the oxidation rates observed, other mechanisms contributing to varying degrees according to temperature and flow rate. An apparently anamolous decrease in reaction rate with increase in flow rate for the O_2-N_2 runs has not been explained but such effects are not unknown and may possibly be due to surface phenomena relating to nucleation and crystal growth.

Langley Research Center,
National Aeronautics and Space Administration,
Langley Station, Hampton, Va., August 11, 1964.

APPENDIX

TEMPERATURE PROFILE SURVEY AND CALIBRATION OF THE OXIDATION FURNACE

The furnace used in this oxidation study was a commercial glow-rod resistance-heated horizontal tube type. Three silicon carbide glow rods were resistance matched and equally spaced around and parallel to the furnace tube. The mullite combustion tube was approximately $1\frac{3}{16}$ inches inside diameter by $1\frac{1}{2}$ inches outside diameter and 22 inches long. The maximum continuous operating temperature rating was 2500° F. The furnace was equipped with a millivolt meter reading temperature directly in Fahrenheit and Centigrade temperatures from a platinum—platinum-rhodium thermocouple whose junction was fixed in the furnace close to the combustion tube. This gage was used to obtain the temperature which hereinafter is designated as the nominal furnace temperature. The temperature-control system provided with the furnace proved to be too coarse to maintain a given temperature within ±15° F required for this study; therefore, a suitable manually controlled autotransformer was substituted and adequate control was thus obtained. In this work the furnace was turned over on its side and supported so that the tube was vertical to allow a specimen to hang freely in the tube when suspended from a balance.

Preliminary measurements using bare thermocouples inside the tube when at a given furnace temperature indicated that there were large variations in temperature according to position and also considerable fluctuations with time at a given position. After various additions and alterations to an air inlet system to the bottom of the tube, a system was found which appeared to give a reasonably uniform hot zone of a size required for this work and with a reasonably uniform air flow in the range of the planned study. The final system consisted of a connection from the compressed-air-line valve to a carbon dioxide absorption bottle, to an anhydrous calcium sulfate filled drying bottle, to a calibrated flow meter, to a small wire-wound tube furnace which was packed with ceramic tubing and operated at 1800° F, through an elbow filled with 3/8-inch-diameter zirconia pebbles, and finally to the lower end of the vertical combustion tube. (See fig. 1.)

With the apparatus described, the survey of the temperature profiles of the oxidation tube was made at various air-flow rates ranging from natural convection (connection at the compressed-air valve broken and the upper end of oxidation tube open) to 0.280 standard ft^3/min for each of furnace temperatures from 1500° F to 2500° F in 100° increments. Temperatures were measured by use of a bare platinum-platinum, 13-percent rhodium thermocouple held rigidly on the end of two-hole refractory ceramic insulator tubing. The tubing was held in a rack and pinion device which allowed the thermocouple junction to be moved vertically in a reproducible manner to various levels inside the furnace tube. The furnace tube was surveyed vertically along its axis in increments of 1 inch. This survey showed a hottest zone which averaged about 5 inches in length for each condition which was called the oxidation zone. Figures 22(a) and 22(b)

show the vertical temperature profile along the axis in the oxidation zone for three flow conditions each at 1500° F and 2500° F nominal furnace temperatures. The thermocouple junction was then moved across the diameter of the tube at the hottest vertical position in approximately 1/4-inch increments. Figures 23(a) and 23(b) show the diametric temperature profiles for nominal furnace temperatures of 1500° F and 2500° F and three flow conditions at the hottest vertical positions. The asymmetric shape of these curves is due to the fact that one end of any diameter will always be closer to a glow rod than the other end. Thus, the temperature profile of the oxidation zone of the furnace was determined for nominal furnace temperature from 1500° F to 2500° F in 100° increments and flow conditions of no forced flow, and for 0.130 and 0.280 standard ft^3/min for each temperature. The survey clearly indicates, as illustrated by figures 22 and 23, that the hot zone is not located at the geometric center of the tube inside the furnace $\left(\text{approximately } 9\frac{1}{3} \text{ inches from top end of tube}\right)$ and rises in the tube with increased air flow. The survey indicated that a temperature variation across the specimen could probably be expected. To determine the magnitude of the temperature variations on the specimen, a 2-centimeter-square platinum sheet 0.002 inch thick with three thermocouples attached was used. The thermocouples were attached one at the center of the square specimen and one each at the upper left and lower right corners. In a manner similar to the one described for the bare thermocouple survey, the specimen was lowered into the tube and maneuvered up and down until the center thermocouple found the hottest point in the oxidation zone. At this position and vertically $\pm 1/2$ inch from this position, all three thermocouples were read and recorded. This procedure was followed for the various air-flow rates and nominal furnace temperature from 1500° F to 2500° F. It was found that the position of least thermal variation was not necessarily coincident with the hottest vertical position. Thus the position to be used for each oxidation condition was determined by raising and lowering the platinum specimen until the position of minimum temperature variation on the specimen was found for each set of temperature and flow conditions to be used in the kinetic runs. The average variation in temperature from center to corner on the specimen was determined to be 12° F, the maximum being 30° F.

At this point it became obvious that the position of a specimen in the furnace tube was a critical condition and that more information was required to be able to specify fully the conditions under which the oxidation kinetic runs were to be made. Ideally, the temperature of the air and specimen should be the same and since the temperatures had been measured in the tube with unshielded thermocouples, it was realized that the true gas temperatures were unknown. Therefore, the gas temperatures were measured for all conditions by use of a shielded, aspirated thermocouple. (See ref. 12.) Figure 24 shows the variation of gas temperature and specimen temperature at four flow rates. The temperature of a platinum specimen and the gas temperatures in the test positions of the furnace were known for a number of nominal furnace temperature settings and several flow rates of air. Once the decision was made to use the temperature of the specimen as the specified test temperature, the next step was to calibrate the furnace so that a given nickel specimen temperature could be reproducibly obtained under any of the flow conditions that were to be used. It was realized that the equilibrium temperature of the nickel specimen would

be somewhat different than that of platinum because of the different radiation characteristics of the surfaces; for example, the platinum retained its luster and was primarily reflective whereas nickel oxidized to a dark absorptive surface. Thus, a test size specimen of nickel with thermocouple attached was positioned in the furnace under conditions previously obtained for the platinum specimen and the nominal furnace temperature adjusted until the nickel specimen attained and held the desired temperature. This procedure was followed for all conditions of flow and temperature to be used in the study and a group of curves were obtained which gave the nominal furnace temperature which was required to give any particular nickel specimen temperature for any of the certain flows of the study. The calibration was spot checked occasionally and rerun whenever a new set of glow rods was installed. There was negligible change in these calibrations during the period when the tests were made. Figure 3 shows a typical group of calibration curves for nickel specimens. This graph shows curves for convective flow, 0.130 and 0.280 standard ft^3/min. Similar curves were found for 0.065 and 0.205 standard ft^3/min and, if plotted, would appear on the figure between the convective flow and 0.130, and 0.130 and 0.280 standard ft^3/min curves, respectively.

REFERENCES

1. Zima, Gordon Everett: Some High Temperature Oxidation Characteristics of Nickel With Chromium Additions. Seventh Tech. Rept. (Contract N6Onr-24430), Dyn. Properties Lab., C.I.T., Apr. 1956.

2. Frederick, S. F.; and Cornet, I.: The Effect of Cobalt on the High Temperature Oxidation of Nickel. J. Electrochem. Soc., vol. 102, no. 6, June 1955, pp. 285-291.

3. Moore, Walter J.; and Lee, James K.: Kinetics of the Formation of Oxide Films on Nickel Foil. Trans. Faraday Soc., vol. 48, 1952, pp. 916-920.

4. Fueki, Kazuo; and Ishibashi, Hirotsugu: Oxidation Studies on Ni-Al Alloys. J. Electrochem. Soc., vol. 108, no. 4, Apr. 1961, pp. 306-311.

5. Kubaschewski, O; and Hopkins, B. E.: Oxidation of Metals and Alloys. Butterworths Sci. Pub. (London), 1953.

6. Gulbransen, E. A.; and Andrew, K. F.: The Kinetics of Oxidation of High Purity Nickel. Jour. Electrochem. Soc., vol. 101, no. 3, Mar. 1954, pp. 128-140.

7. Moore, Walter J.; and Lee, James K.: Oxidation Kinetics of Nickel and Cobalt. J. Chem. Phys., vol. 19, no. 2, Feb. 1951, p. 255.

8. Lawless, Kenneth R.; Young, Fred W., Jr.; and Gwathmey, Allan T.: L'oxydation D'un Monocristal De Nickel. J. Chim. Phys., t. 53, no. 8, 1956, pp. 667-674.

9. Smith, Joseph, ed.: X-Ray Powder Data File - Sets 1-5 (Revised). Spec. Tech. Publ. 48-J, Am. Soc. Testing Mater., c.1960, p. 582.

10. Hauffe, K.: Reactions In and On Solids. AEC-tr-4495, U.S. At. Energy Comm., July 1962.

11. Hauffe, K.: Investigations on the Oxidation of Metals as a Tool for the Exploration of the Movement of Ions in Solid Oxides. Kinetics of High-Temperature Processes, W. D. Kingery, ed., Technol. Press of M.I.T. and John Wiley & Sons, Inc., c. 1959, pp. 282-293.

12. Mullikin, H. F.: Gas-Temperature Measurement and the High-Velocity Thermocouple. Temperature - Its Measurement and Control In Science and Industry, vol. I, Reinhold Publ. Corp., 1941, pp. 775-804.

TABLE I.- VOLUME AND LINEAR FLOW RATES

FOR KINETIC RUNS AT INDICATED

SPECIMEN TEMPERATURES

Volume flow rate, ft^3/min	Linear flow rate, ft/sec
Specimen temperature, 1500° F	
0.065	0.587
.130	1.06
.205	1.56
.280	1.97
Specimen temperature, 1750° F	
0.065	0.668
.130	1.23
.205	1.82
.280	2.31
Specimen temperature, 2000° F	
0.065	0.757
.130	1.40
.205	2.08
.280	2.66
Specimen temperature 2250° F	
0.065	0.843
.130	1.58
.205	2.34
.280	3.02
Specimen temperature, 2500° F	
0.065	0.934
.130	1.76
.205	2.62
.280	3.64

TABLE II.- PARABOLIC RATE CONSTANT FOR NICKEL OXIDATION

AT SPECIFIED AIR-FLOW RATES AND SPECIMEN TEMPERATURES

Flow rate (air), standard ft^3/min	Parabolic rate constant, k_p, $g^2cm^{-4}sec^{-1}$	Average parabolic rate constant, $\bar{k}_p$, $g^2cm^{-4}sec^{-1}$
	Specimen temperature, 1500° F	
Convective*	2.01×10^{-11}	2.01×10^{-11}
0.065	1.65	
.065	1.91	
.130	2.40	
.205	1.73	
.205	2.02	
.280	2.33	
	Specimen temperature, 1750° F	
Convective*	1.45×10^{-10}	1.52×10^{-10}
0.065	1.62	
.130	1.47	
.205	1.41	
.280	1.63	
	Specimen temperature, 2000° F	
Convective*	8.03×10^{-10}	7.46×10^{-10}
0.065	7.54	
.130	7.73	
.205	6.68	
.280	7.32	
	Specimen temperature, 2250° F	
Convective*	3.54×10^{-9}	3.37×10^{-9}
0.065	3.49	
.130	3.15	
.205	3.12	
.280	3.57	
	Specimen temperature, 2500° F	
Convective*	1.50×10^{-8}	1.41×10^{-8}
0.065	1.40	
.130	1.39	
.205	1.37	
.280	1.41	

*No forced air flow, system open to air at both ends.

TABLE III.- PARABOLIC RATE CONSTANTS FOR NICKEL OXIDATION FOR OXYGEN-NITROGEN RUNS AT DESIGNATED CONDITIONS

Specimen temperature, ^{o}F	Parabolic rate constant, k_p, $g^2cm^{-4}sec^{-1}$, for flow rates of -	
	0.130 standard ft^3/min	0.280 standard ft^3/min
Oxygen partial pressure, 380 mm Hg		
1750	1.35×10^{-10}	1.22×10^{-10}
2000	8.75	8.27
2250	42.0	41.0
2500	150	153
Oxygen partial pressure, 76 mm Hg		
1750	1.30×10^{-10}	1.20×10^{-10}
2000	8.00	7.42
2250	36.5	34.2
2500	126	119
Oxygen partial pressure, 38 mm Hg		
1750	1.17×10^{-10}	1.08×10^{-10}
2000	7.19	6.55
2250	32.4	29.1
2500	113	99.5
Oxygen partial pressure, 7.6 mm Hg		
1750	1.02×10^{-10}	8.05×10^{-11}
2000	5.90	48.5
2250	25.2	213
2500	83.8	715

TABLE IV.- VALUES OF n OBTAINED FROM PLOT OF VARIATIONS OF LOG k_p WITH LOG p_{O_2}

Specimen temperature, °F	Values of n obtained for flow rate of -	
	0.130 standard ft^3/min	0.280 standard ft^3/min
1750	9.52	5.61
2000	7.28	5.37
2250	6.19	4.94
2500	5.56	4.66
Average	7.14	5.14

TABLE V.- COLOR OF SPECIMEN OUTER OXIDE SURFACE AND SUBSURFACE OXIDE AT INDICATED CONDITIONS FOR O_2-N_2 MIXTURE RUNS

Gas flow rate, standard ft^3/min	Oxygen partial pressure, mm Hg	Color of -	
		Outer surface	Subsurface
Specimen temperature, 1750° F			
0.130	7.6	Green cast	
.130	38	Green cast	
.130	76	Green cast	
.130	380	Green cast	
.280	7.6	Green cast	
.280	38	Green cast	
.280	76	Green cast	
.280	380	Green cast	
Specimen temperature, 2000° F			
0.130	7.6	Green cast	Gray-green
.130	38	Green cast	Gray-green
.130	76	Green cast	Gray-green
.130	380	Green cast	Gray-green
.280	7.6	Green cast	Gray-green
.280	38	Green cast	Gray-green
.280	76	Green cast	Gray-green
.280	380	Green cast	Gray-green
Specimen temperature, 2250° F			
0.130	7.6	Gray	Light green
.130	38	Gray	Light green
.130	76	Gray	Light green
.130	380	Gray	Light green
.280	7.6	Gray	Light green
.280	38	Gray	Light green
.280	76	Gray	Light green
.280	380	Gray	Light green
Specimen temperature, 2500° F			
0.130	7.6	Dark gray*	Light green
.130	38	Dark gray*	Light green
.130	76	Dark gray*	Light green
.130	380	Dark gray*	Light green
.280	7.6	Dark gray*	Light green
.280	38	Dark gray*	Light green
.280	76	Dark gray*	Light green
.280	380	Dark gray*	Light green

*These oxide surfaces were rough, whereas the others were fairly smooth.

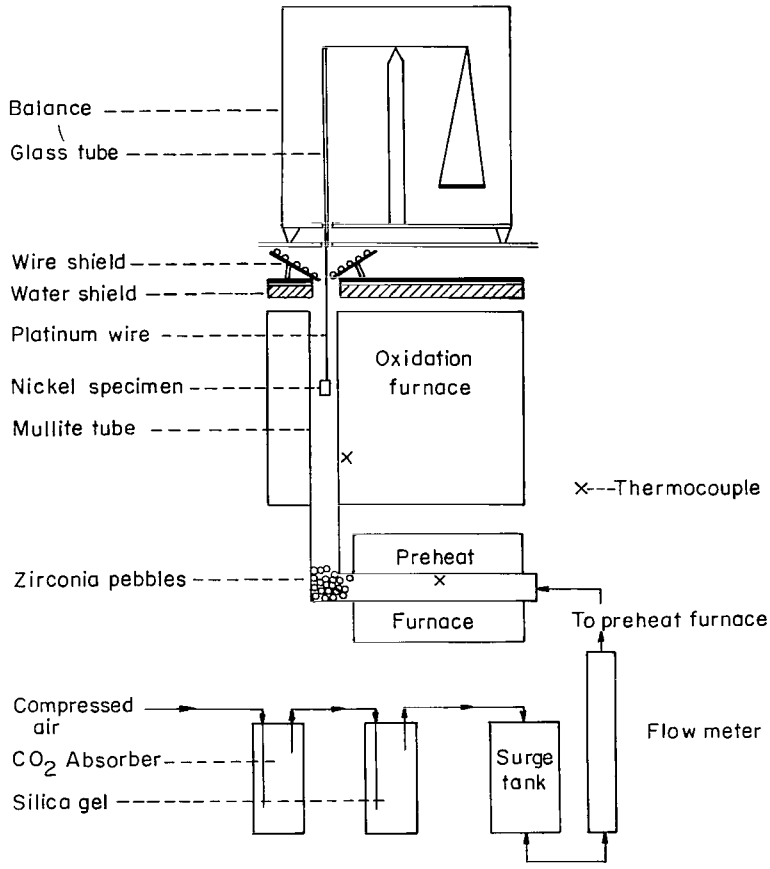

(a) Gas train used for nickel oxidation studies using air.

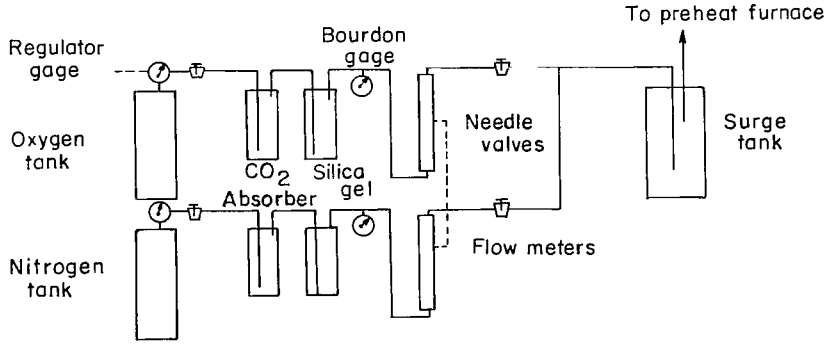

(b) Gas train used for mixing oxygen and nitrogen gases for nickel oxidation studies of varying O_2 partial pressures.

Figure 1.- Schematic drawing showing thermobalance and associated apparatus used in kinetic oxidation studies.

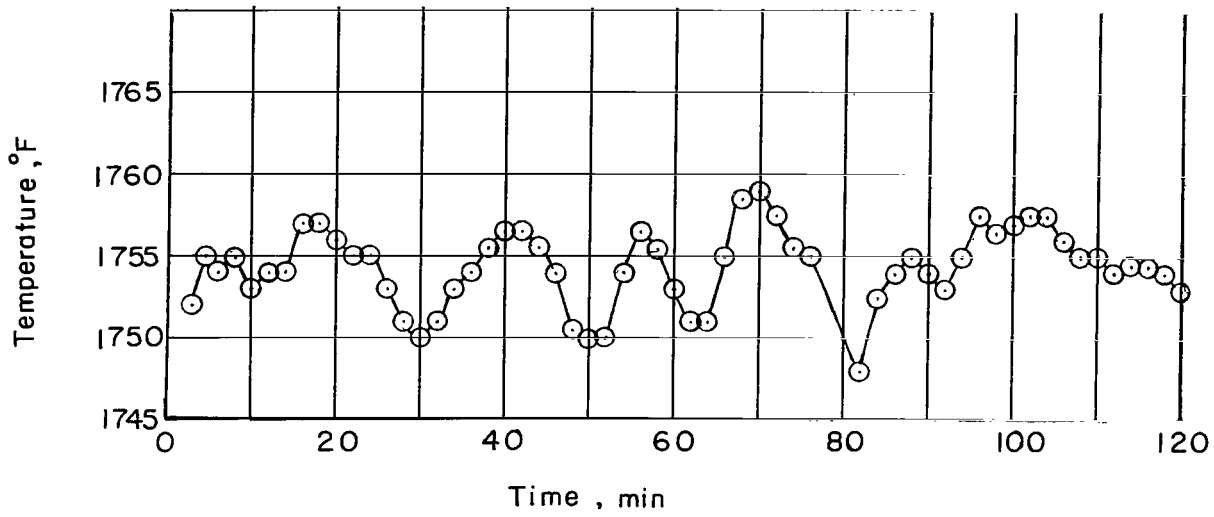

(a) For specimen temperature of 1750° F (averaged 1754° F).

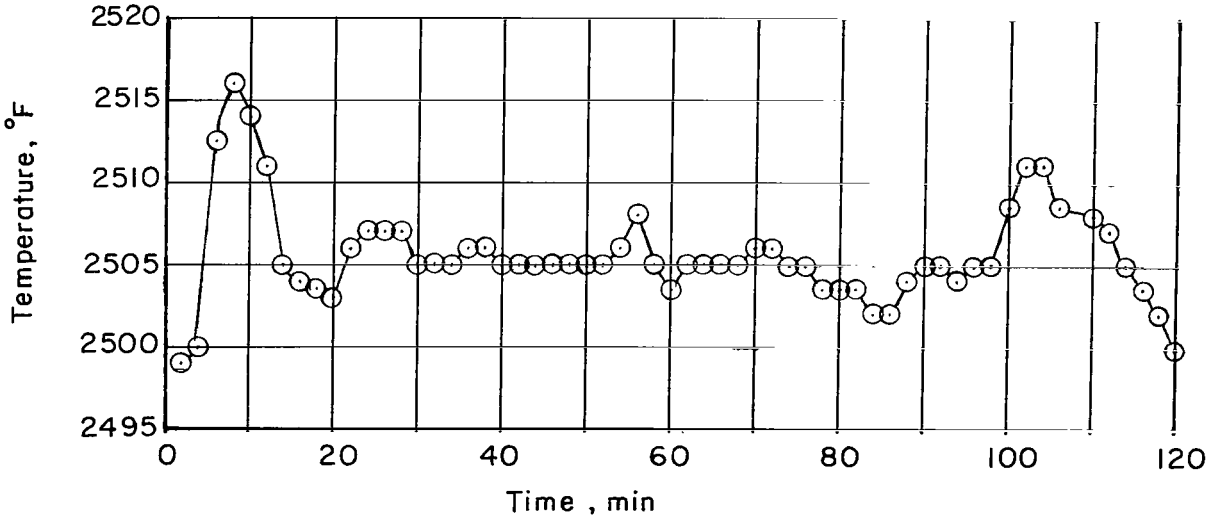

(b) For specimen temperature of 2500° F (averaged 2505° F).

Figure 2.- Variation of specimen temperature with time for a typical kinetic oxidation run lasting 2 hours.

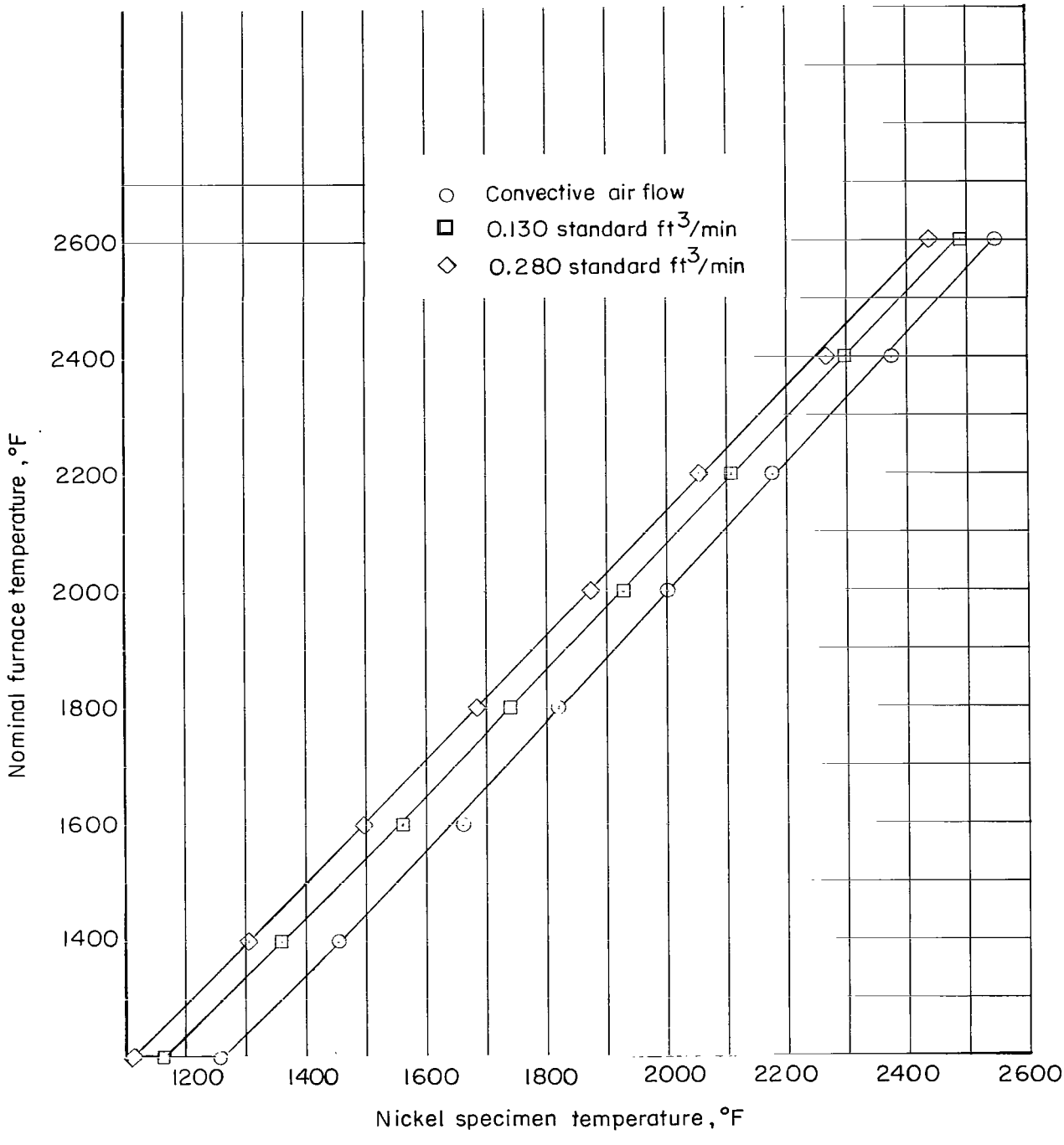

Figure 3.- Typical calibration curves of nominal furnace temperature with nickel specimen temperature. 1800° F preheater temperature.

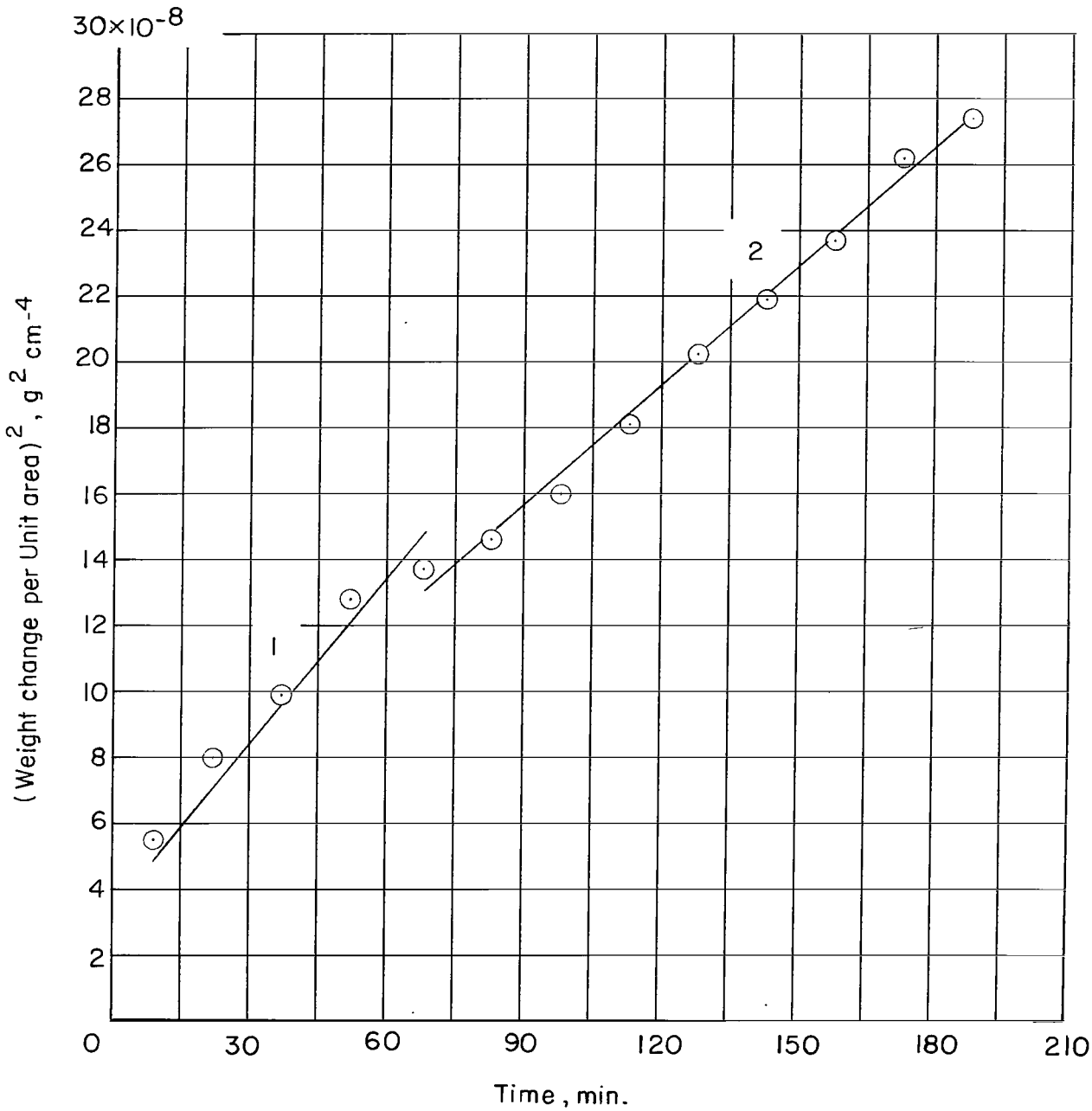

Figure 4.- Parabolic oxidation curve for nickel at 1500° F specimen temperature and convective air flow. Slope 1; $k_p = 2.78 \times 10^{-11}$ $g^2cm^{-4}sec^{-1}$. Slope 2; $k_p = 2.01 \times 10^{-11}$ $g^2cm^{-4}sec^{-1}$.

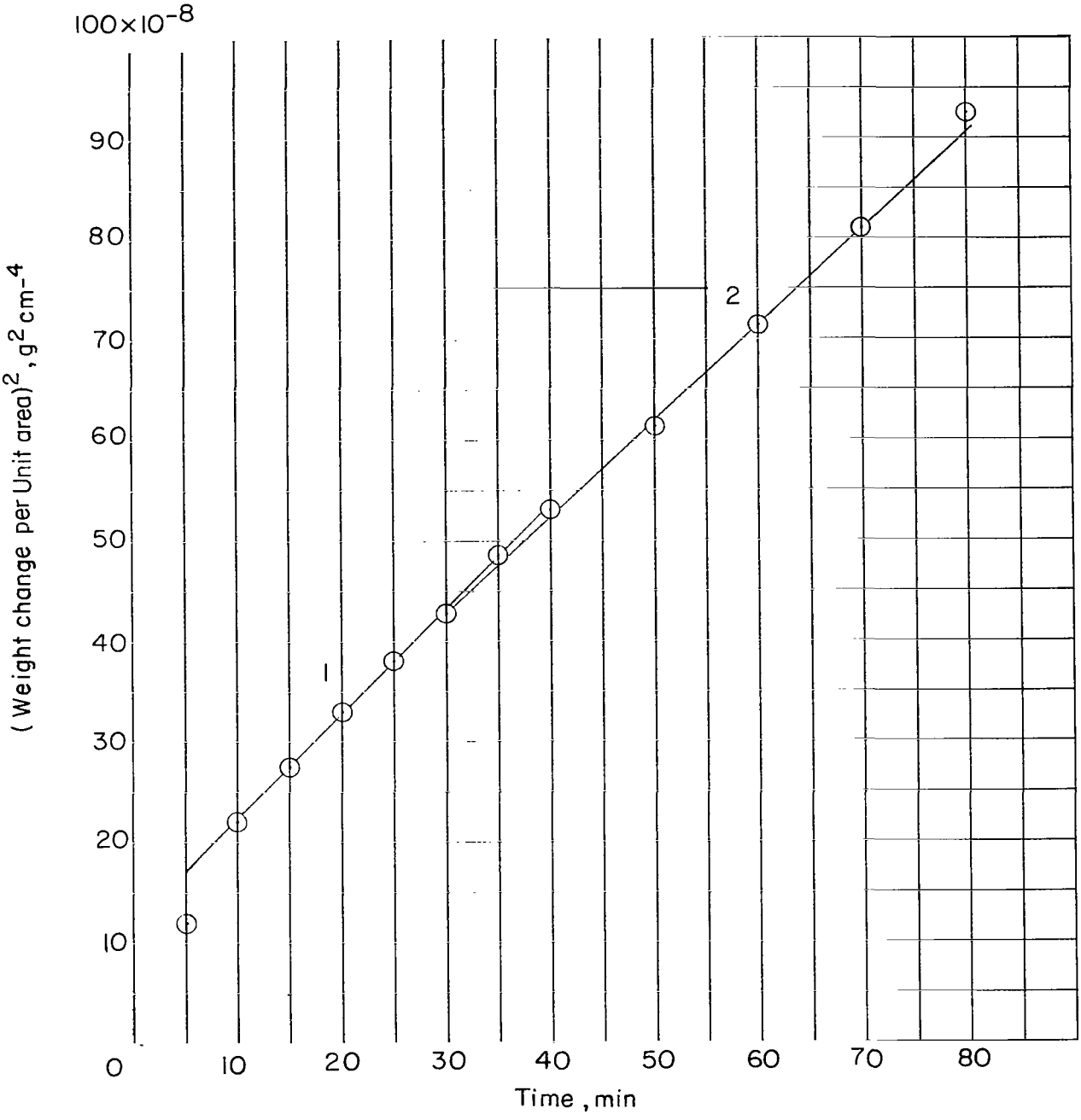

Figure 5.- Parabolic oxidation curve for nickel at 1750° F specimen temperature and 0.065 standard ft^3/min air flow rate. Slope 1; $k_p = 1.72 \times 10^{-10}$ $g^2cm^{-4}sec^{-1}$. Slope 2; $k_p = 1.62 \times 10^{-10}$ $g^2cm^{-4}sec^{-1}$.

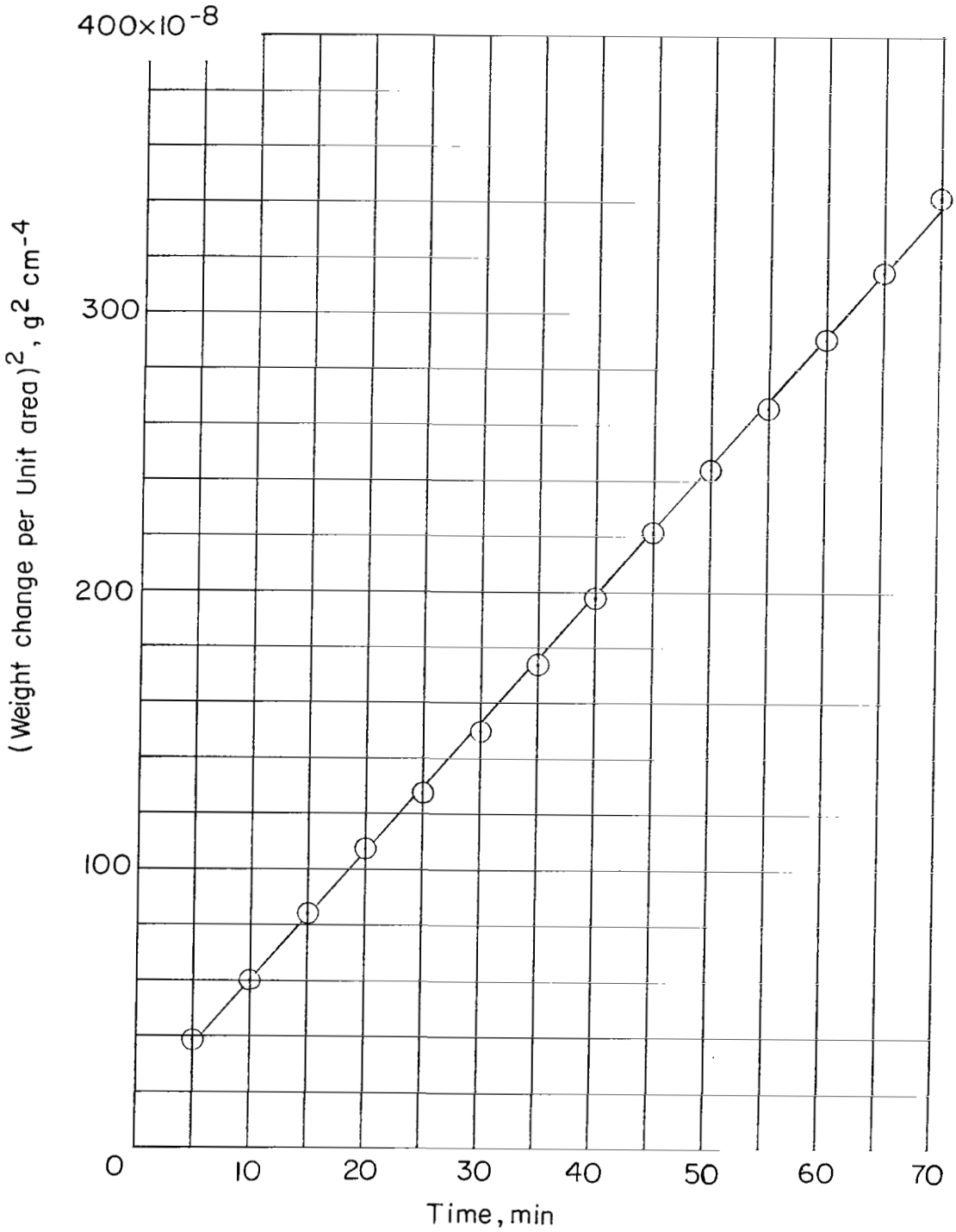

Figure 6.- Parabolic oxidation curve for nickel at 2000° F specimen temperature and 0.130 standard ft^3/min air flow rate. $k_p = 7.73 \times 10^{-10}$ $g^2cm^{-4}sec^{-1}$.

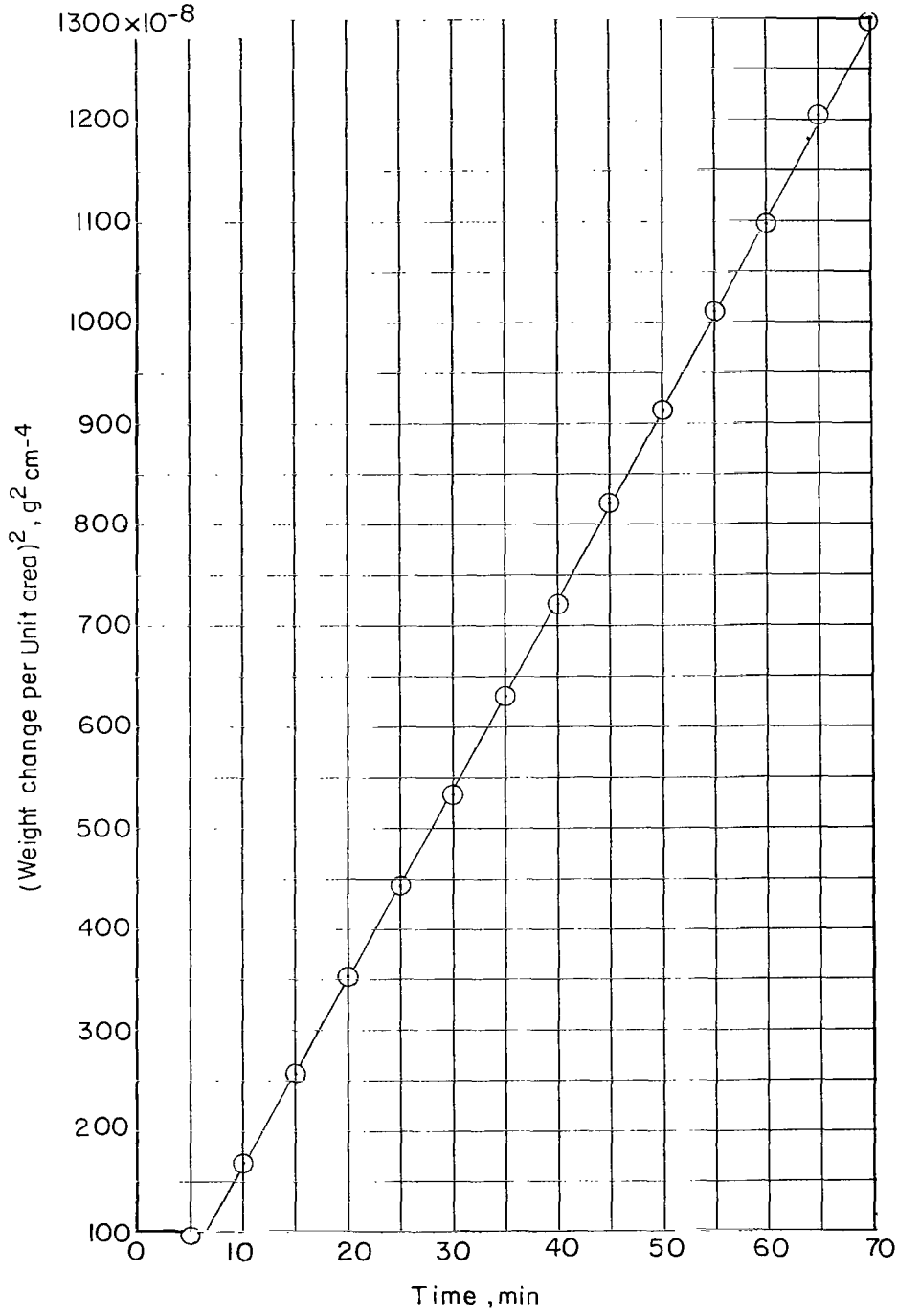

Figure 7.- Parabolic oxidation curve for nickel at 2250° F specimen temperature and 0.205 standard ft^3/min air flow rate. $k_p = 3.12 \times 10^{-9}\ g^2cm^{-4}sec^{-1}$.

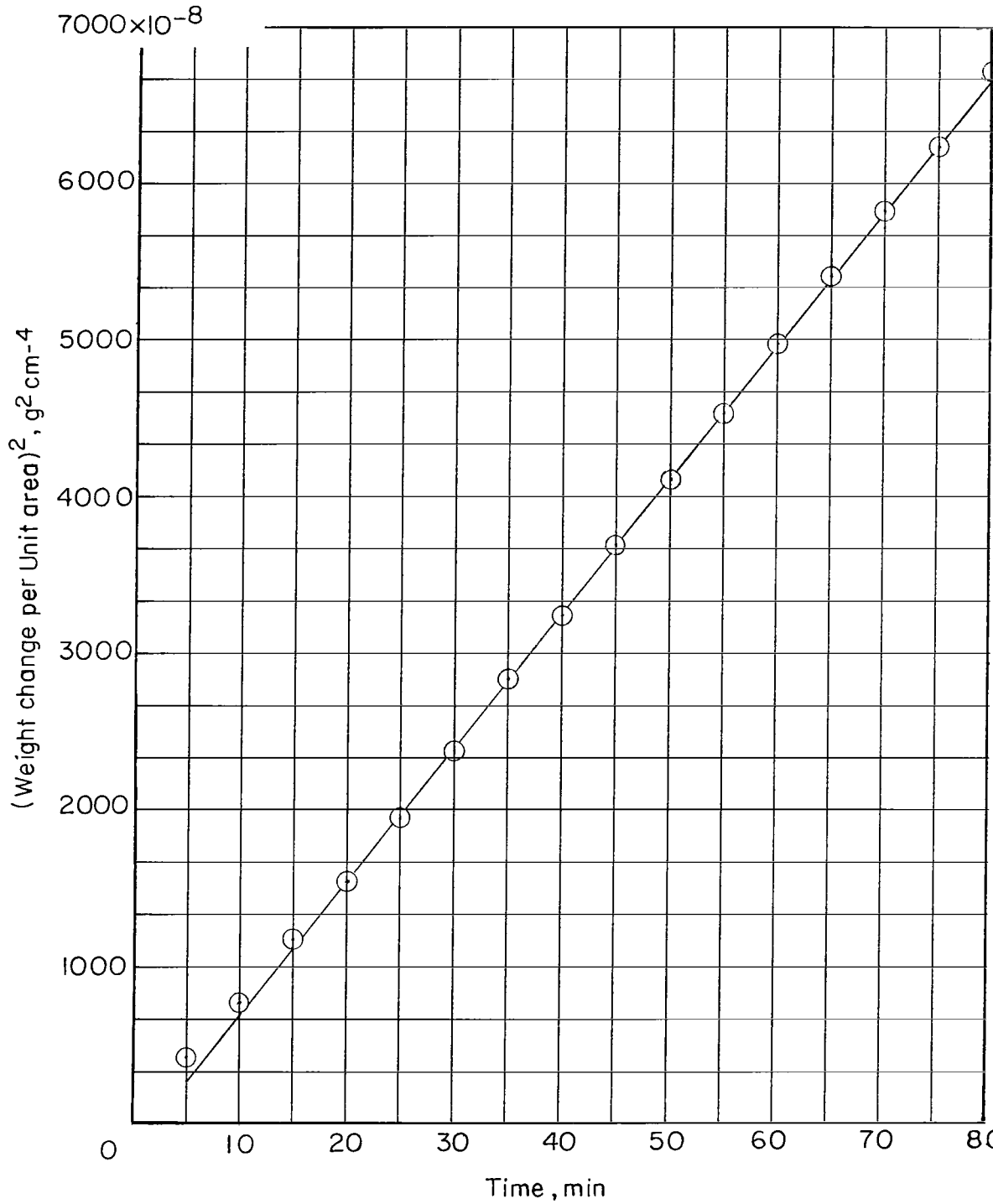

Figure 8.- Parabolic oxidation curve for nickel at 2500° F specimen temperature and 0.280 standard ft^3/min air flow rate. $k_p = 1.41 \times 10^{-8}$ $g^2cm^{-4}sec^{-1}$.

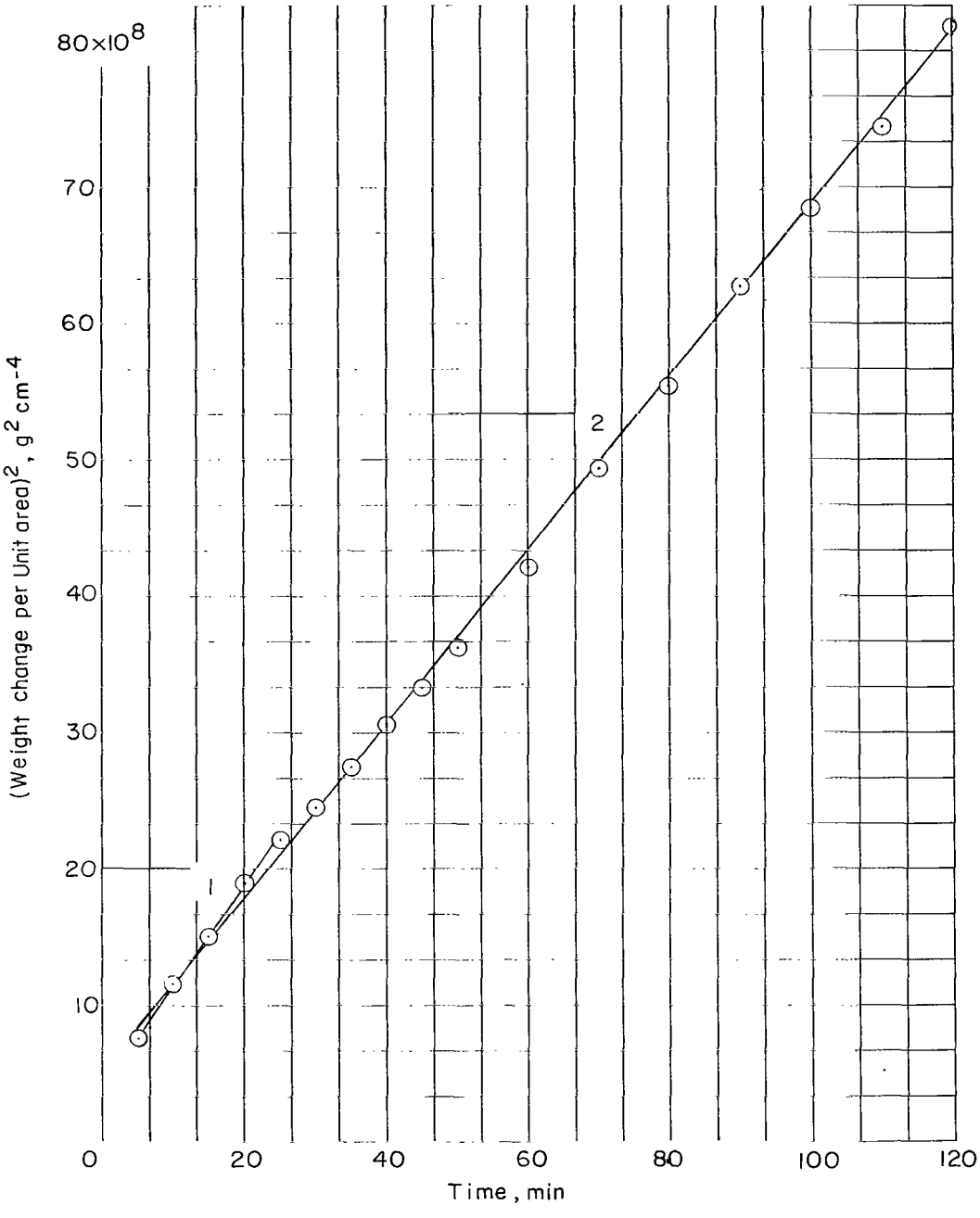

Figure 9.- Parabolic oxidation curve for nickel at 1756° F specimen temperature, 7.6 mm Hg oxygen partial pressure, and 0.130 standard ft^3/min gas flow rate. Slope 1; $k_p = 1.21 \times 10^{-10}$ $g^2cm^{-4}sec^{-1}$. Slope 2; $k_p = 1.05 \times 10^{-10}$ $g^2cm^{-4}sec^{-1}$.

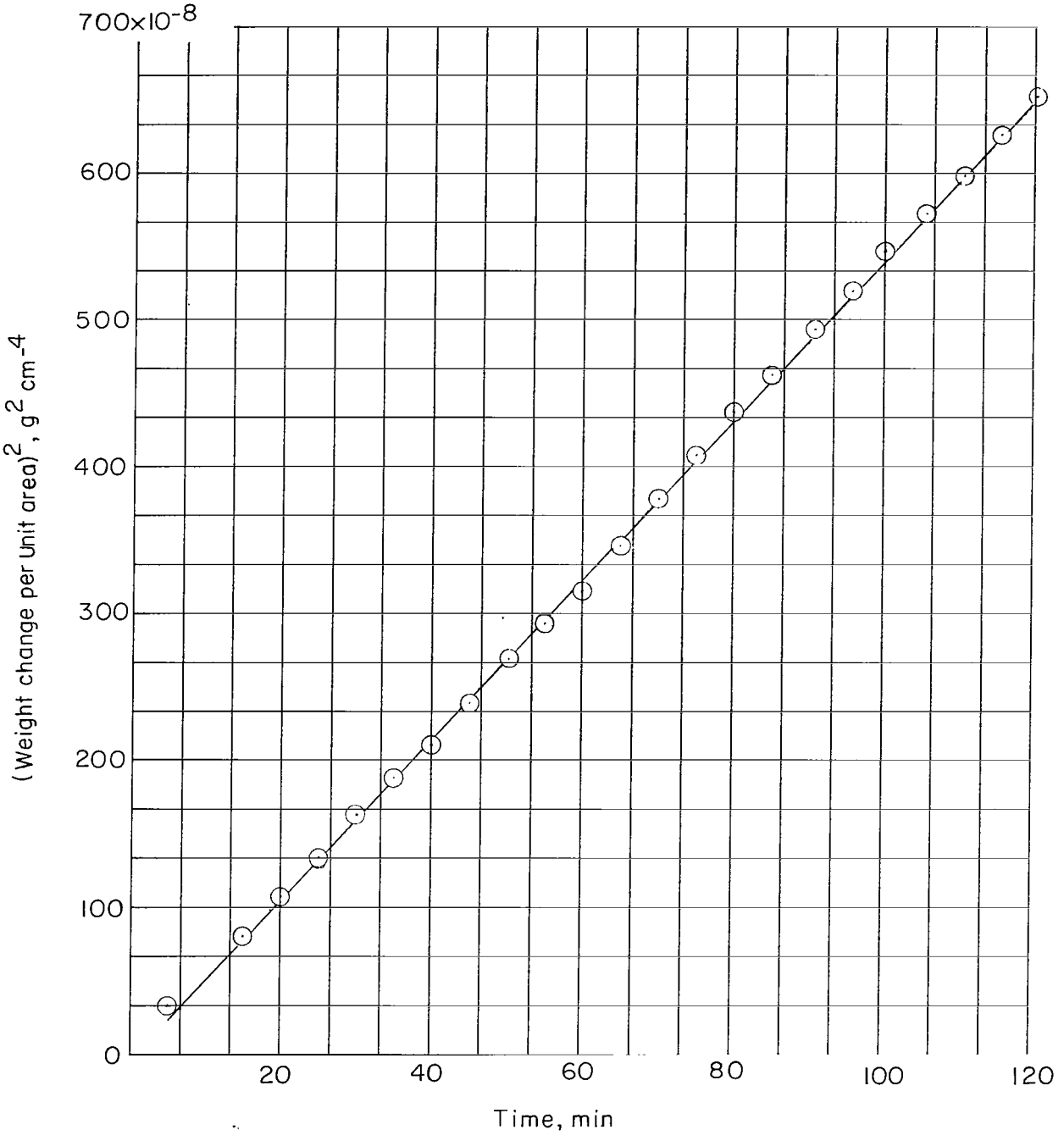

Figure 10.- Parabolic oxidation curve for nickel at 2007° F specimen temperature, 38 mm Hg oxygen partial pressure, and 0.130 standard ft^3/min gas flow rate. $k_p = 9.08 \times 10^{-10}\ g^2cm^{-4}sec^{-1}$.

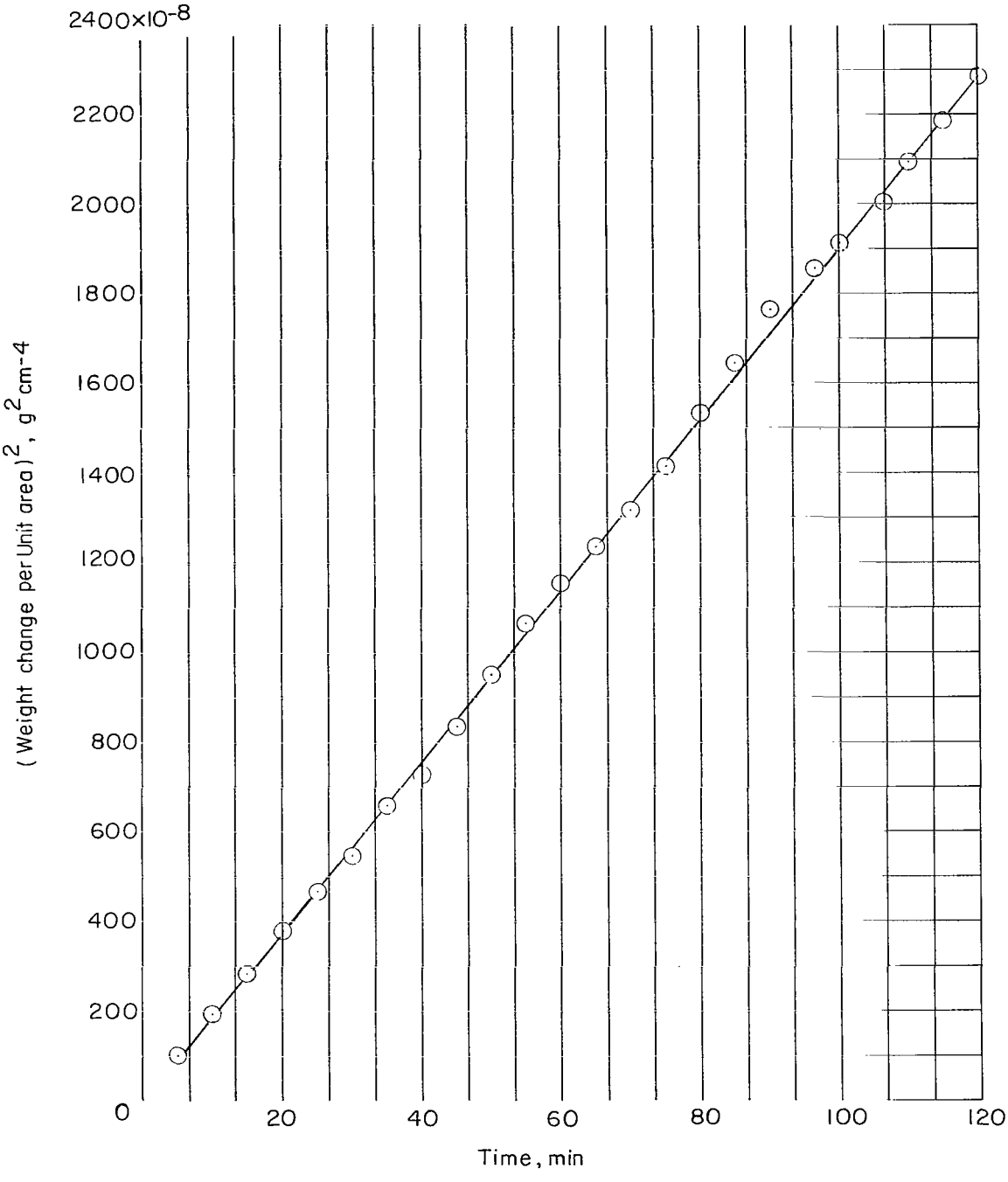

Figure 11.- Parabolic oxidation curve for nickel at 2242° F specimen temperature, 76 mm Hg oxygen partial pressure, and 0.280 standard ft^3/min gas flow rate. $k_p = 3.19 \times 10^{-9}\ g^2cm^{-4}sec^{-1}$.

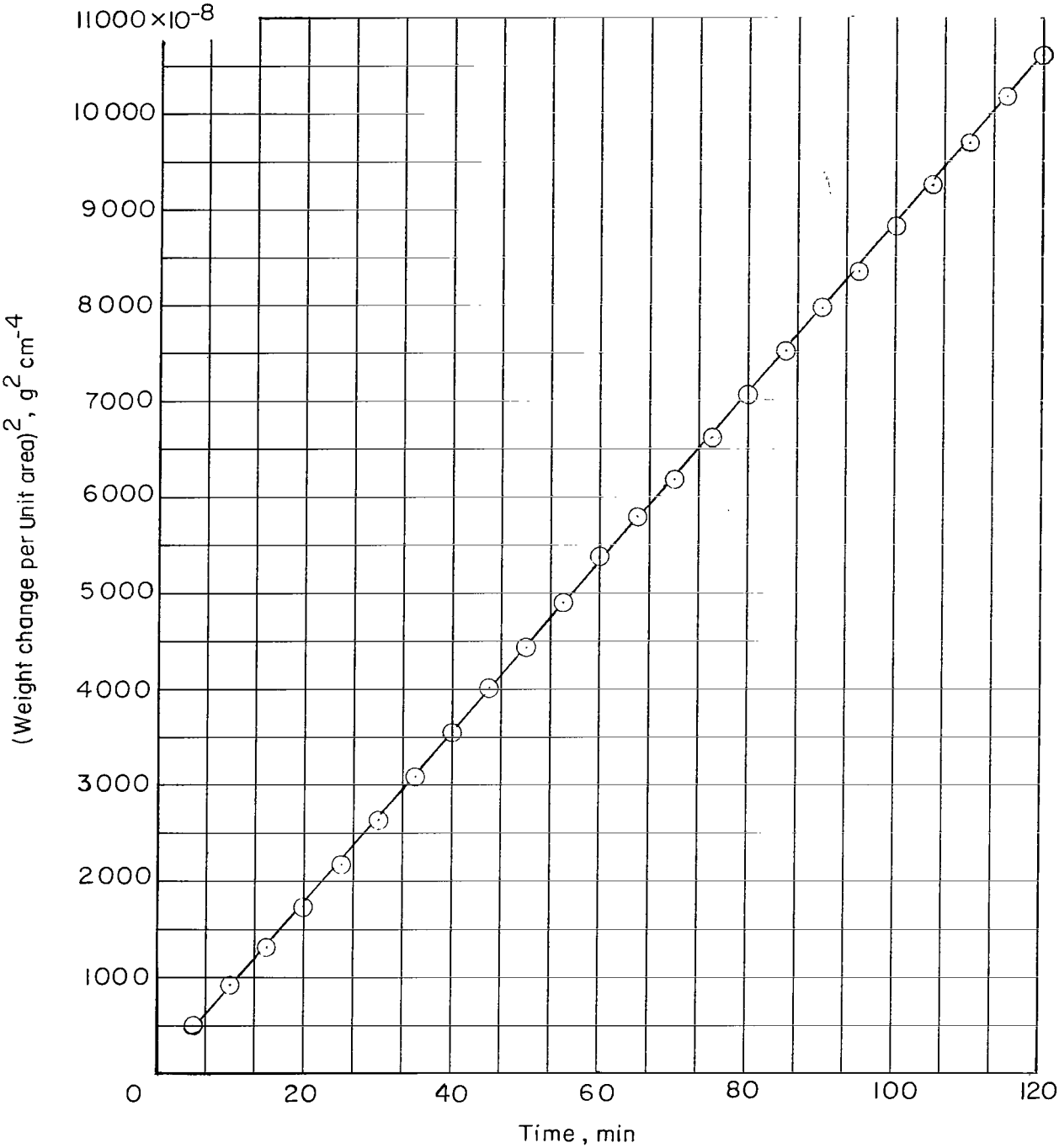

Figure 12.- Parabolic oxidation curve for nickel at 2485° F specimen temperature, 380 mm Hg oxygen partial pressure, and 0.280 standard ft^3/min gas flow rate. $k_p = 1.47 \times 10^{-8}\ g^2cm^{-4}sec^{-1}$.

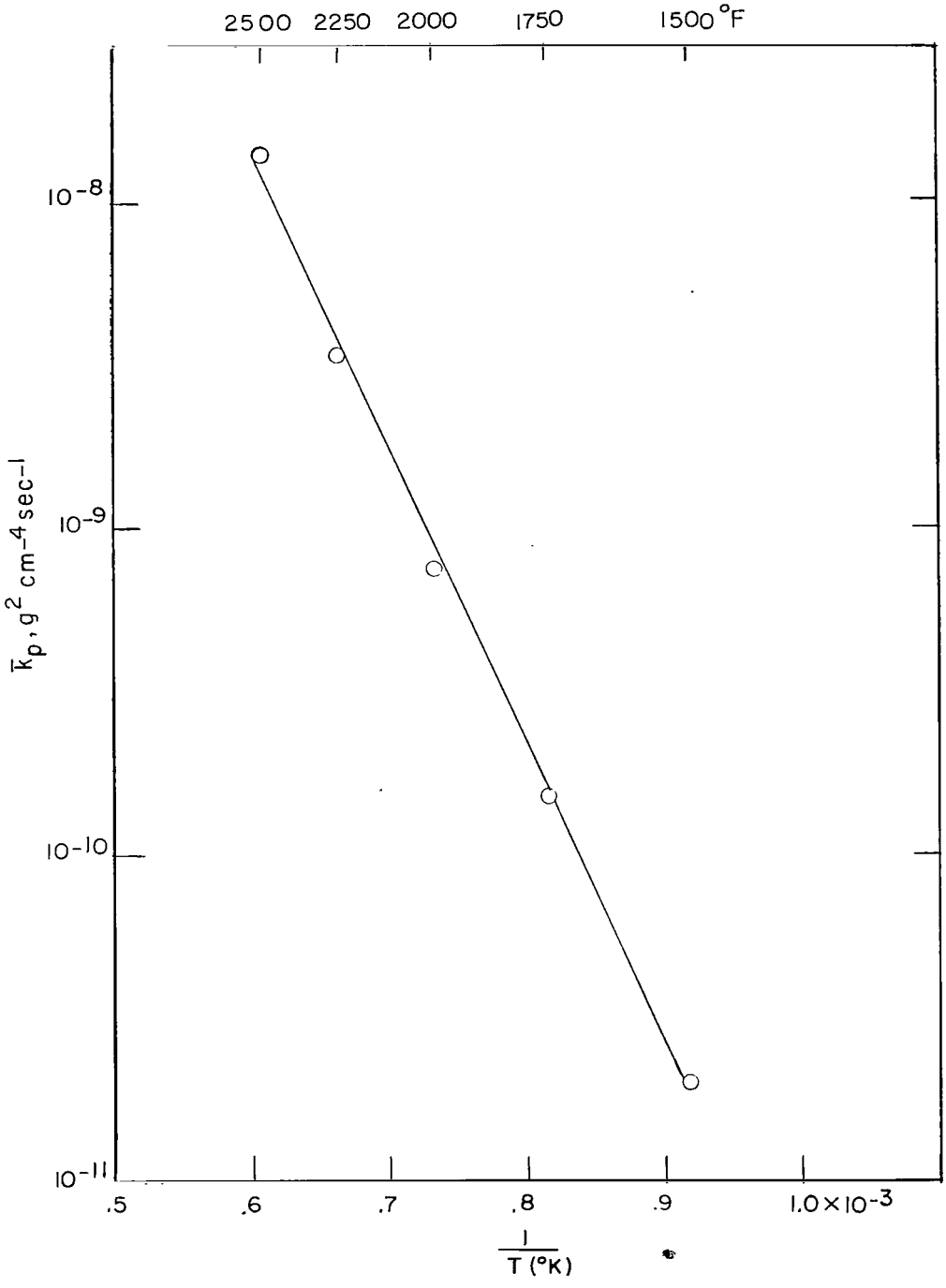

Figure 13.- Arrhenius plot of average flow parabolic reaction rate constant $\bar{k}_p$ for nickel oxidation using air at specimen temperatures of 1500° F, 1750° F, 2000° F, 2250° F, and 2500° F.

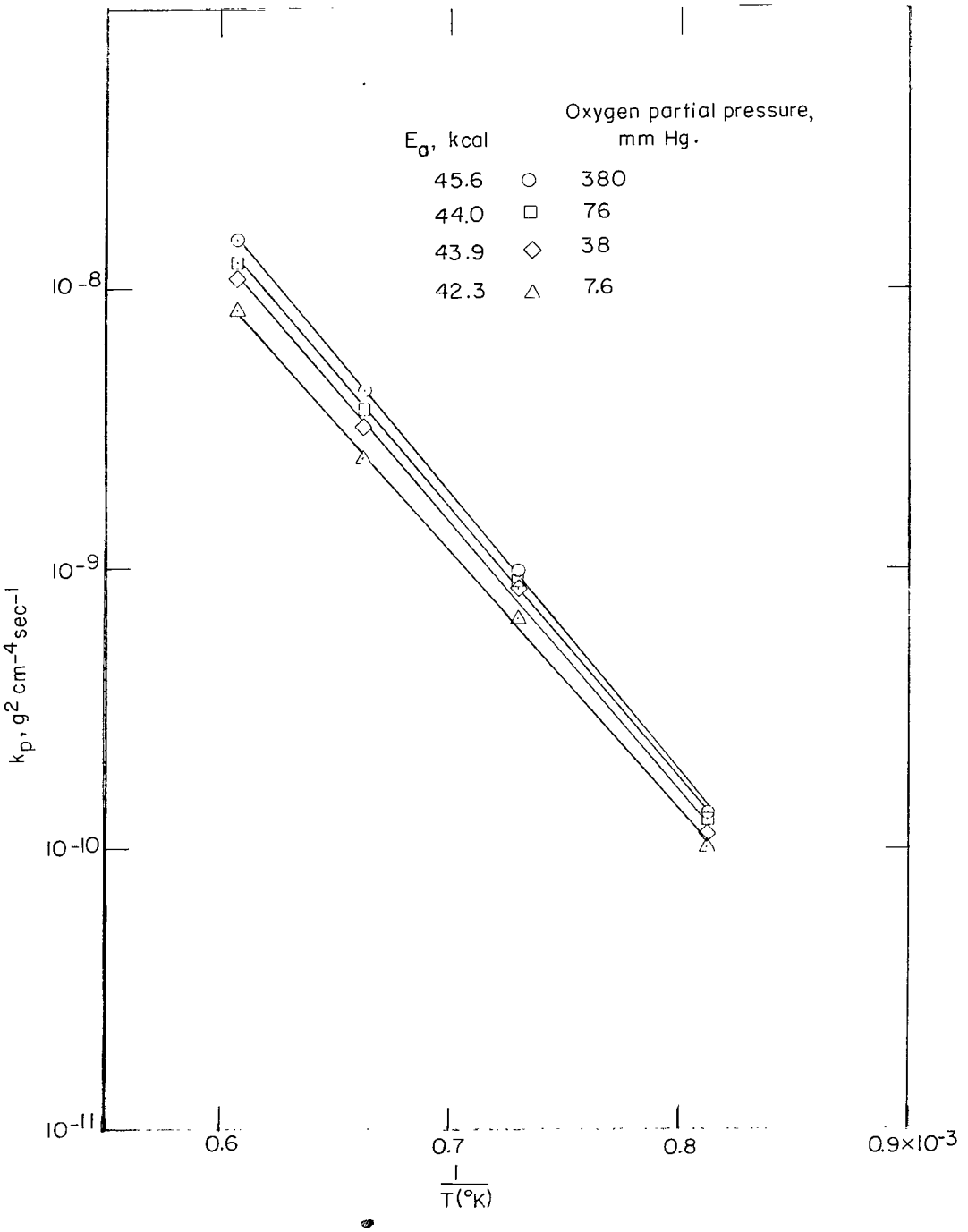

(a) 0.130 standard ft^3/min gas flow rate.

Figure 14.- Temperature dependence of parabolic rate constant for 7.6, 38, 76, and 380 mm Hg oxygen partial pressure.

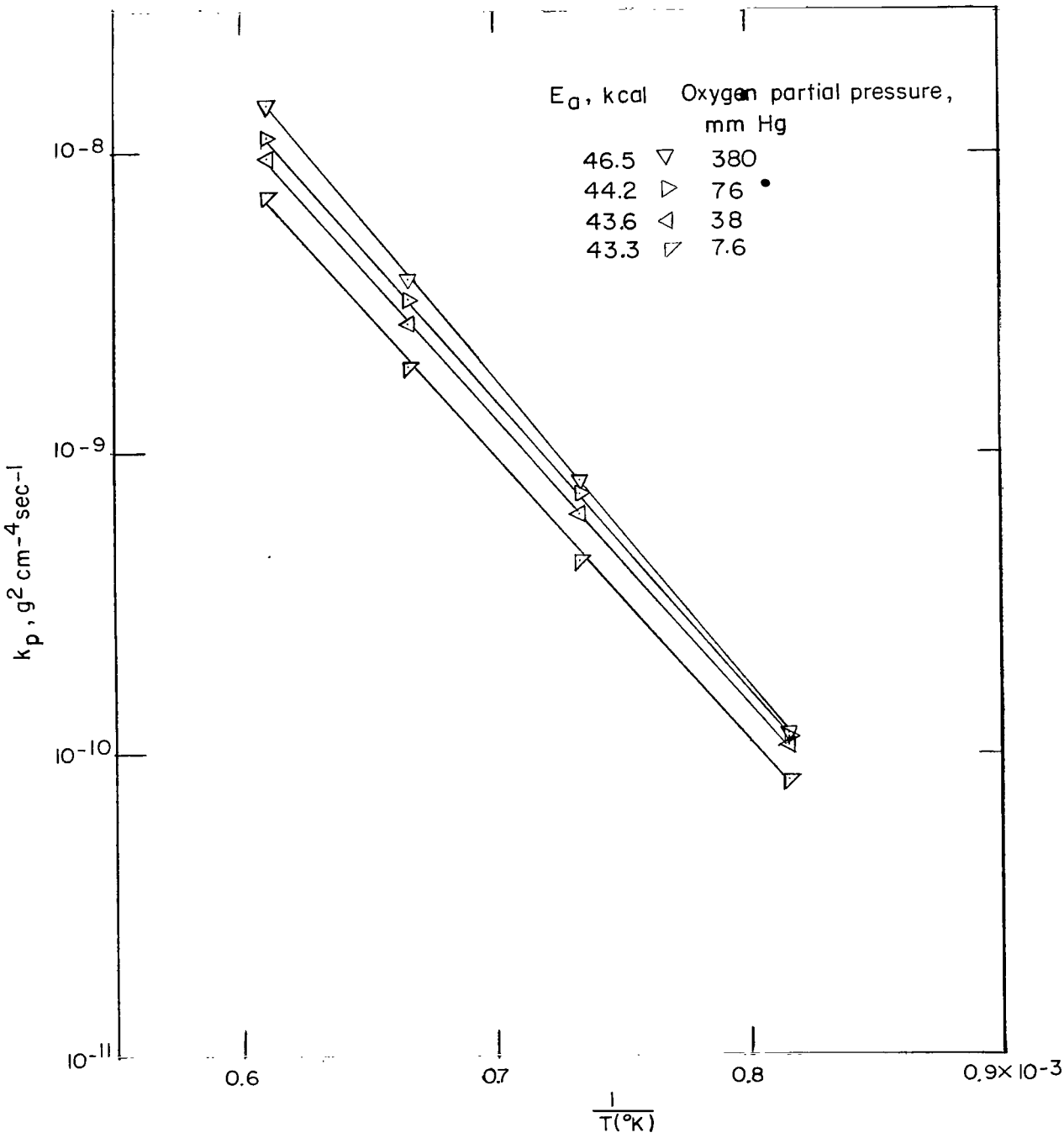

(b) 0.280 standard ft^3/min gas flow rate.

Figure 14.- Concluded.

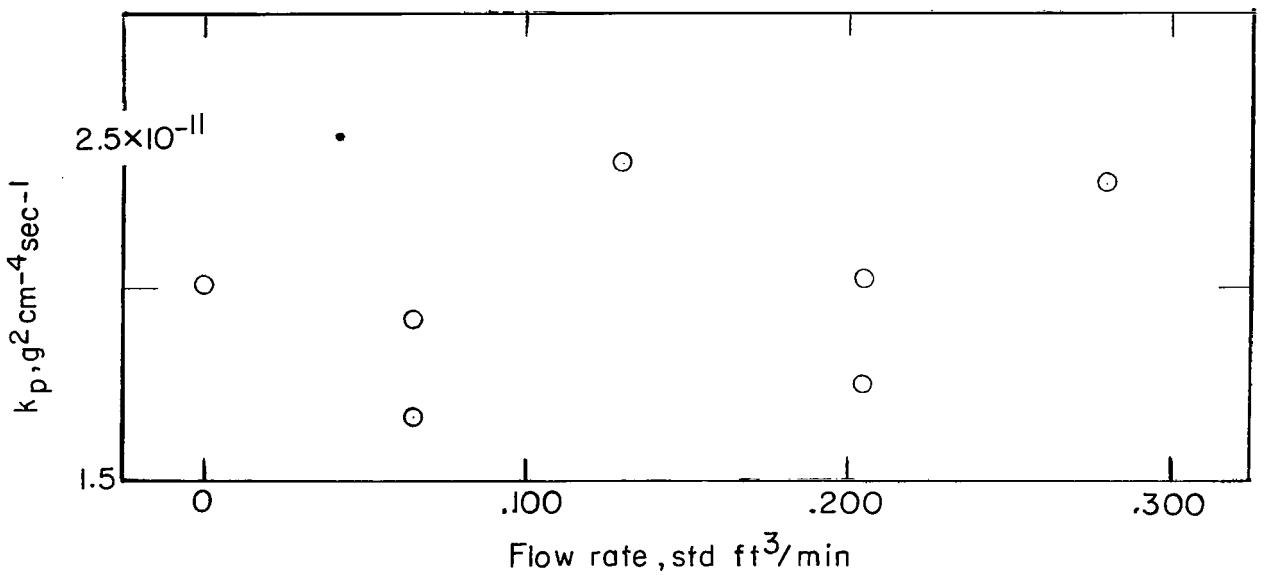

(a) 1500° F.

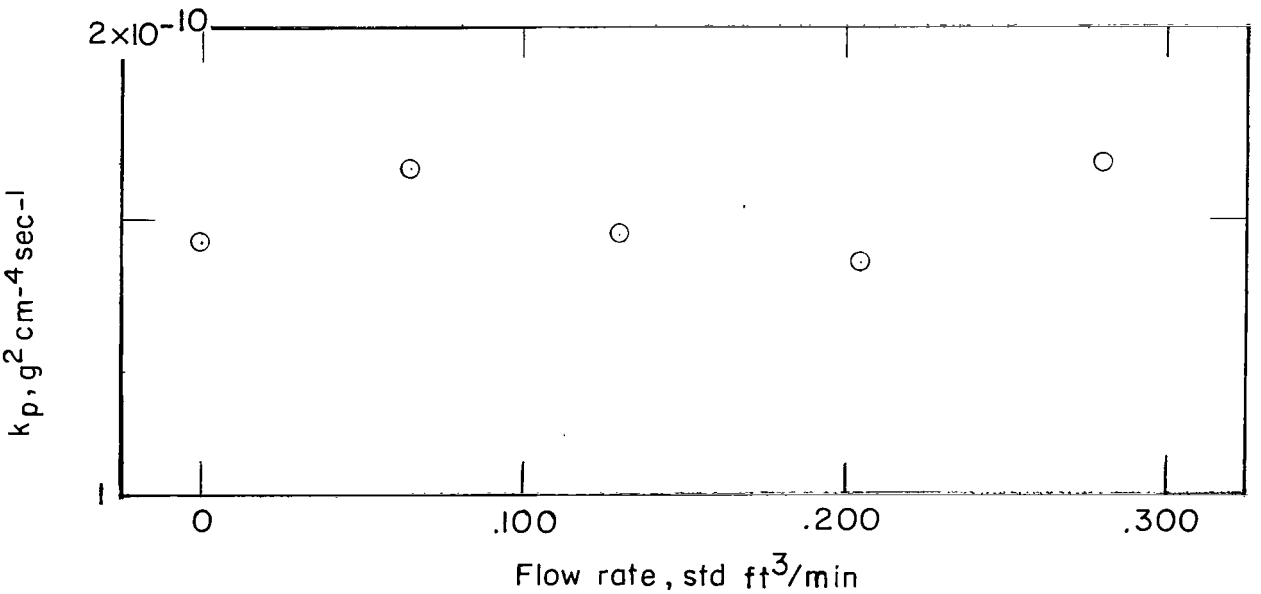

(b) 1750° F.

Figure 15.- Experimental k_p for five air flow rates and temperatures.

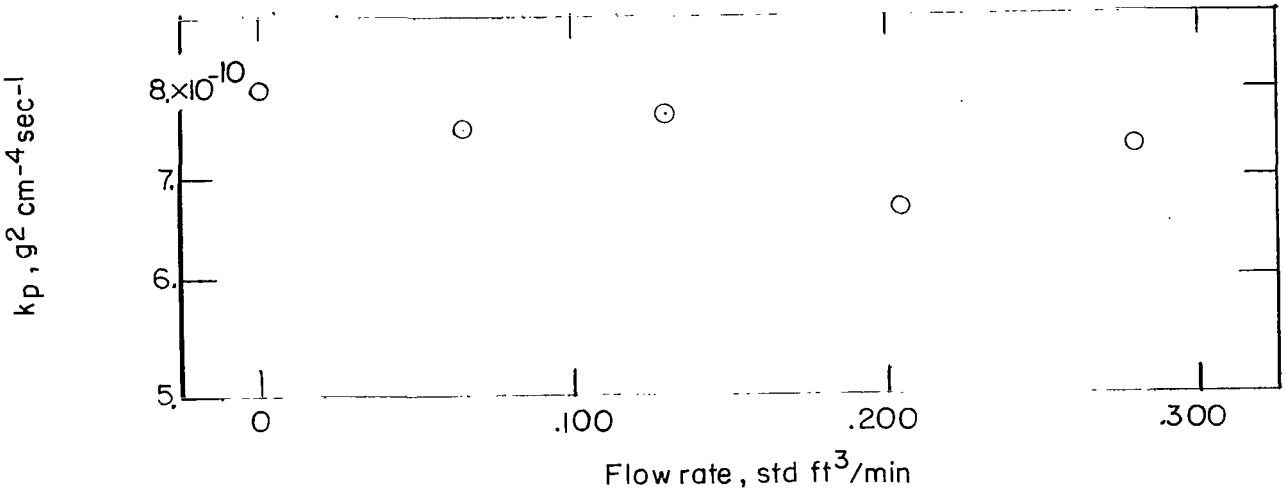

(c) 2000° F.

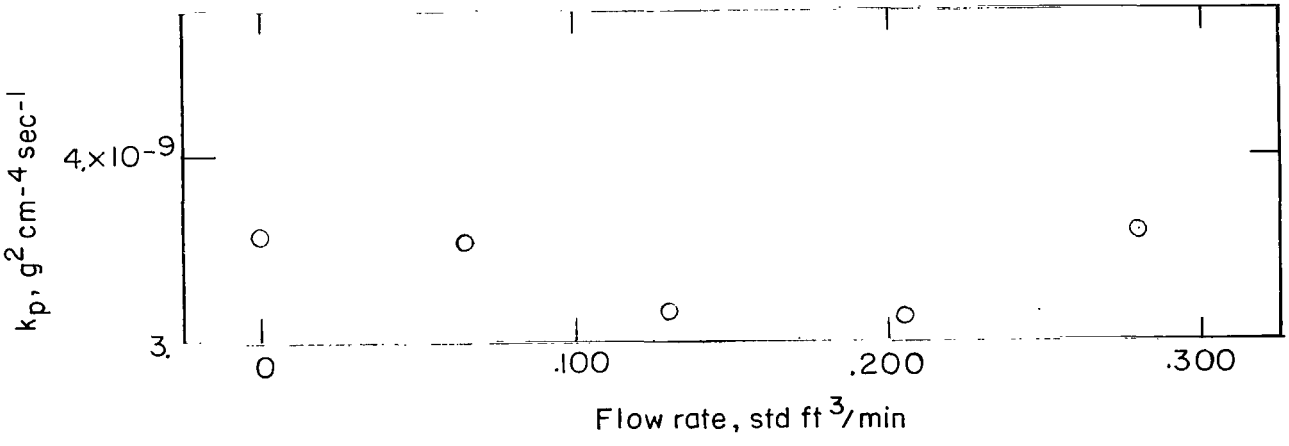

(a) 2250° F.

Figure 15.- Continued.

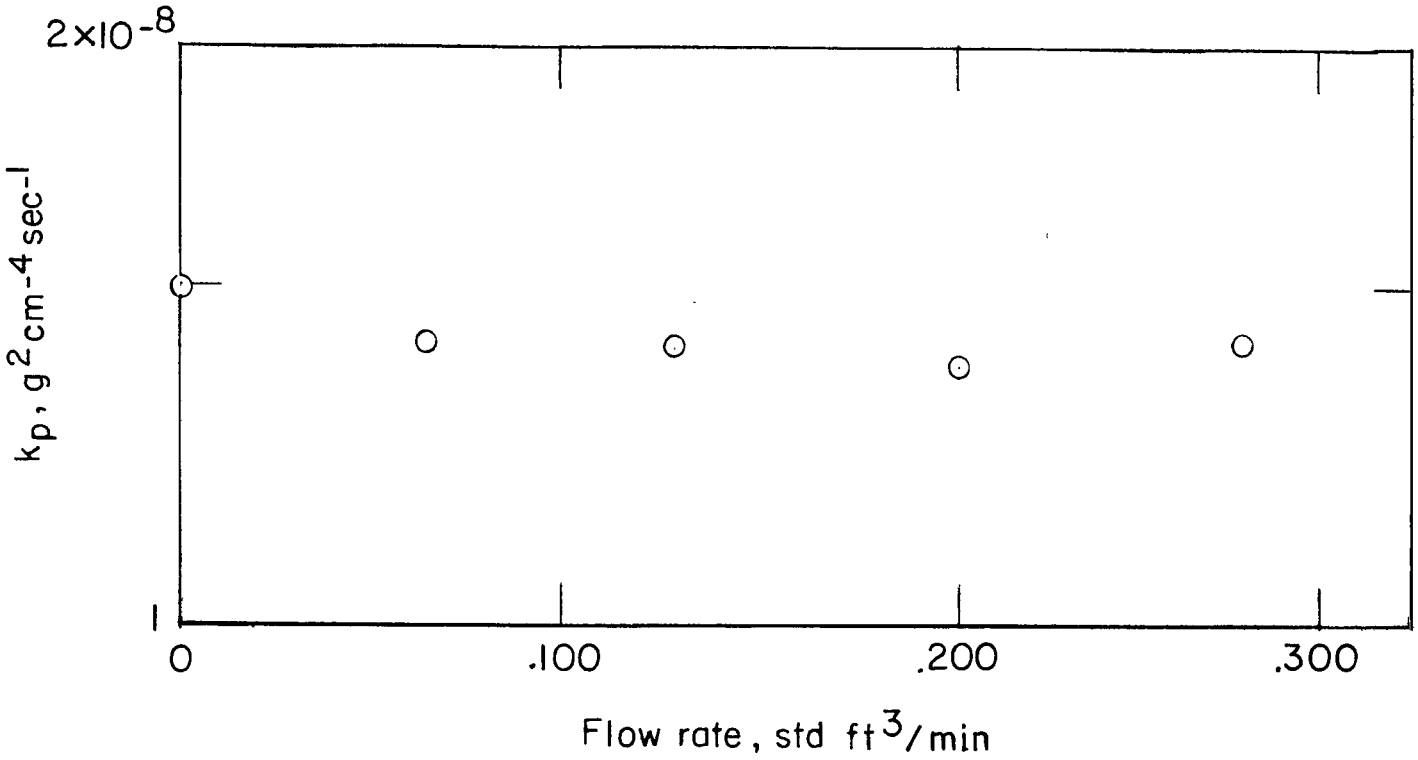

(e) 2500° F.

Figure 15.- Concluded.

	Investigators	Ref. no.	E_a, kcal/mole	Ni Purity, %	O_2 Pressure, mm Hg.
○	Zima	1	45.1	99.95	760
□	Frederick & Cornet	2	51.0	99.9 Carbonyl Ni	152 (air)
◇	Fueki & Ishibashi	4	28.4	99.98 Electrolytic Ni	150 (air)
△	Gulbransen & Andrew	6	41.2	99.99	76
◿	Present study		41.3	99.5 ± 0.3	159 (air)

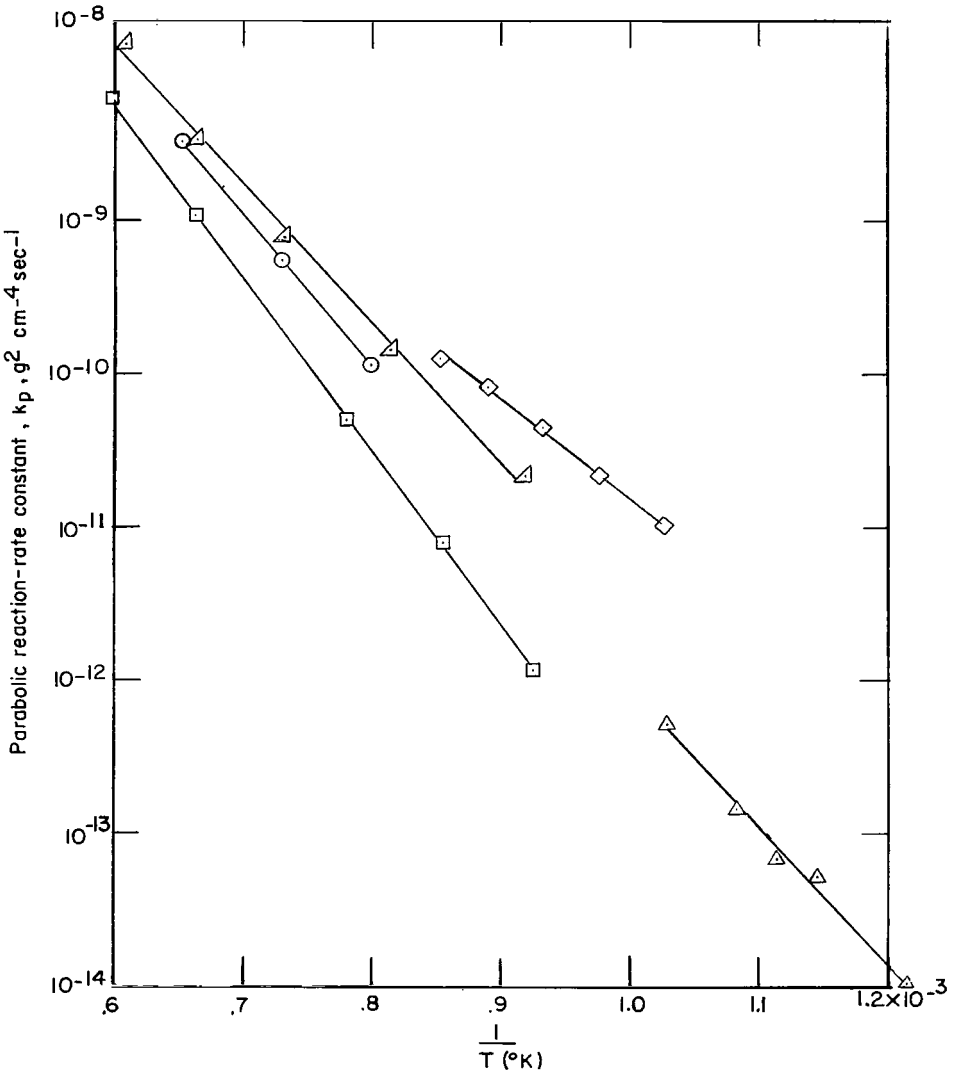

Figure 16.- Arrhenius plot of $\bar{k}_p$ for the present study as compared with other investigations.

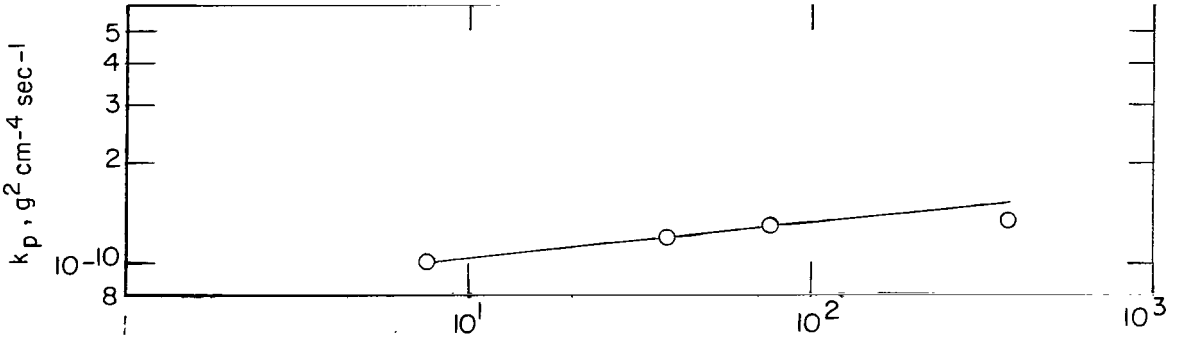

(a) 1750° F, 0.130 standard ft^3/min.

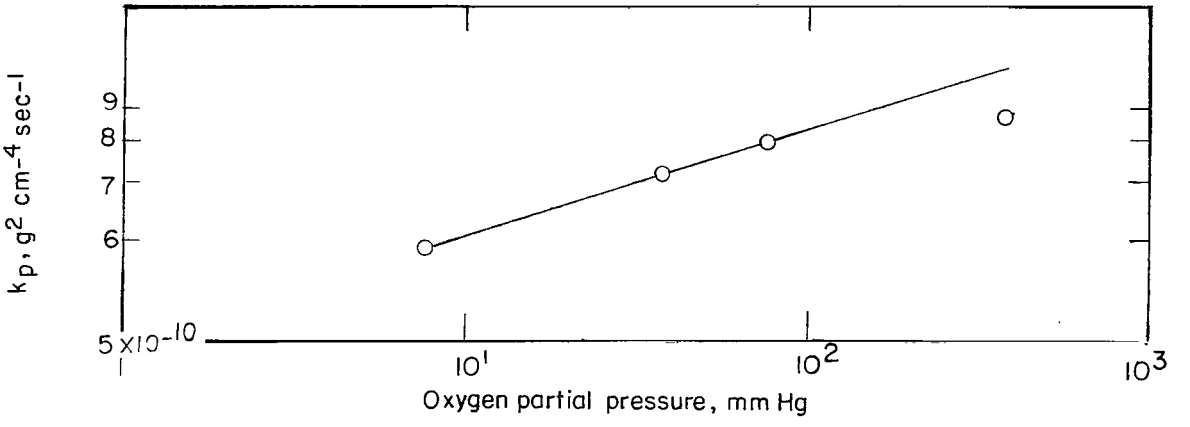

(b) 2000° F, 0.130 standard ft^3/min.

Figure 17.- Variation of k_p with oxygen partial pressure for indicated cases of specimen temperature and gas flow rate.

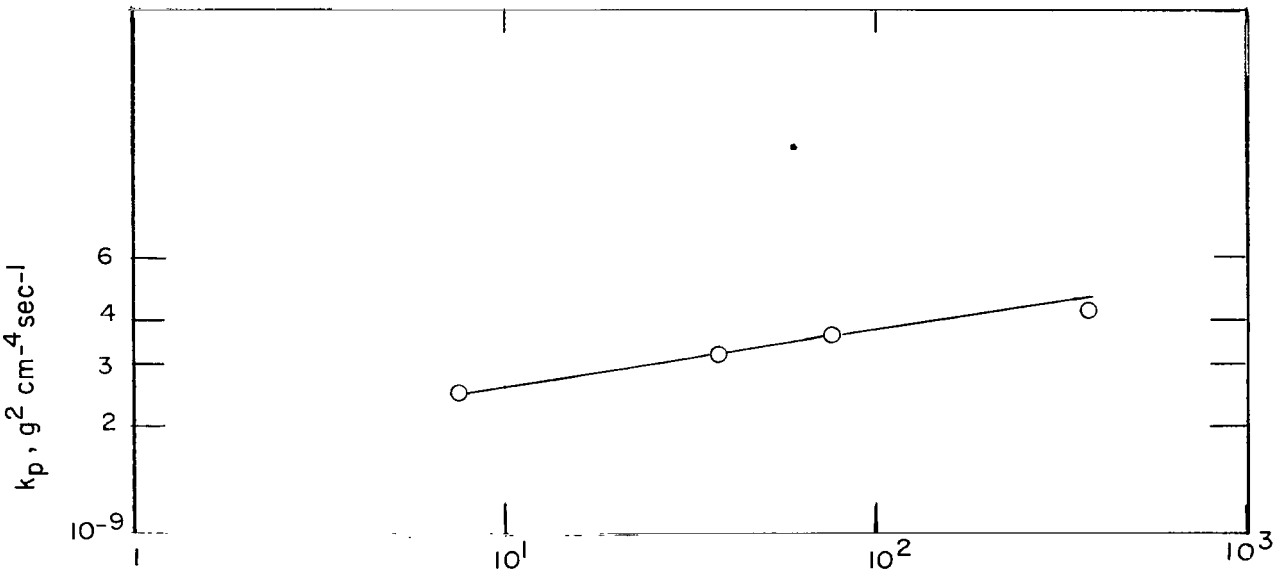

(c) 2250° F, 0.130 standard ft^3/min.

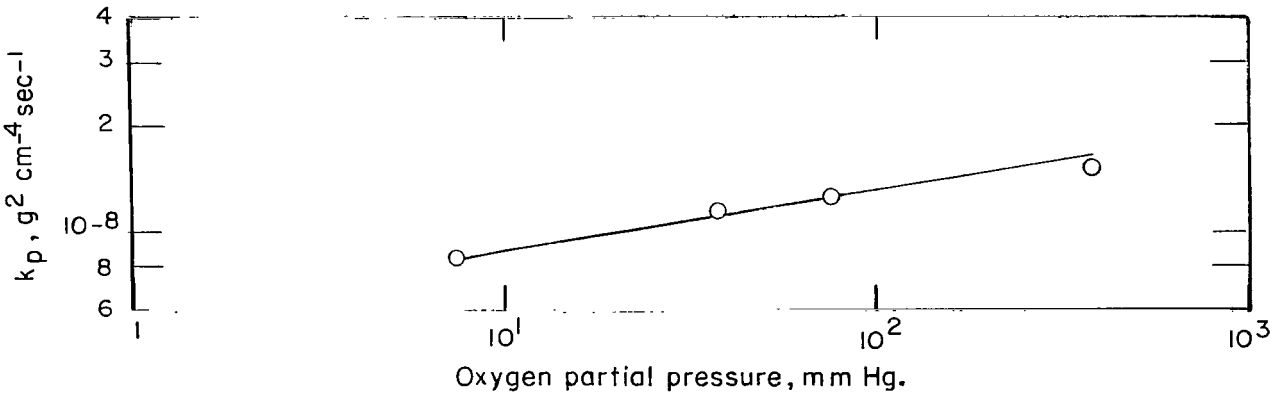

(d) 2500° F, 0.130 standard ft^3/min.

Figure 17.- Continued.

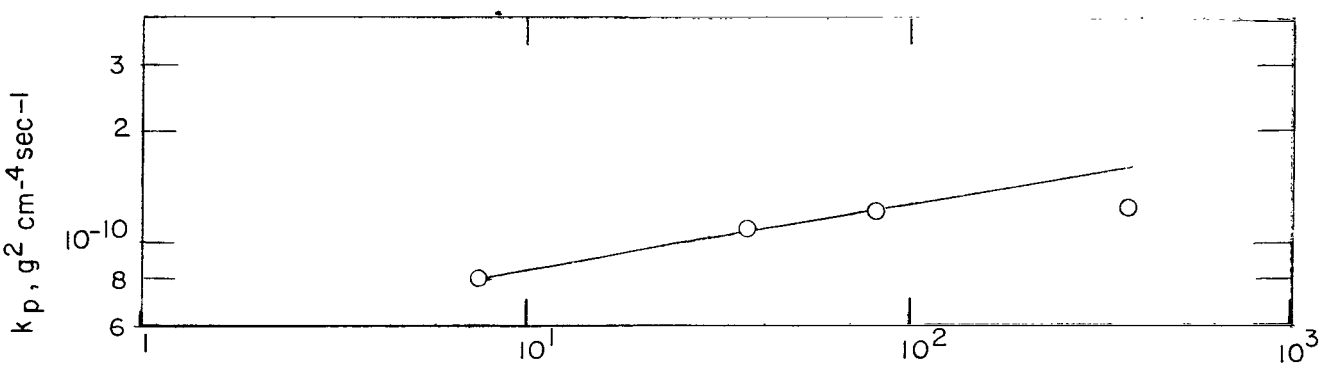

(e) 1750° F, 0.280 standard ft^3/min.

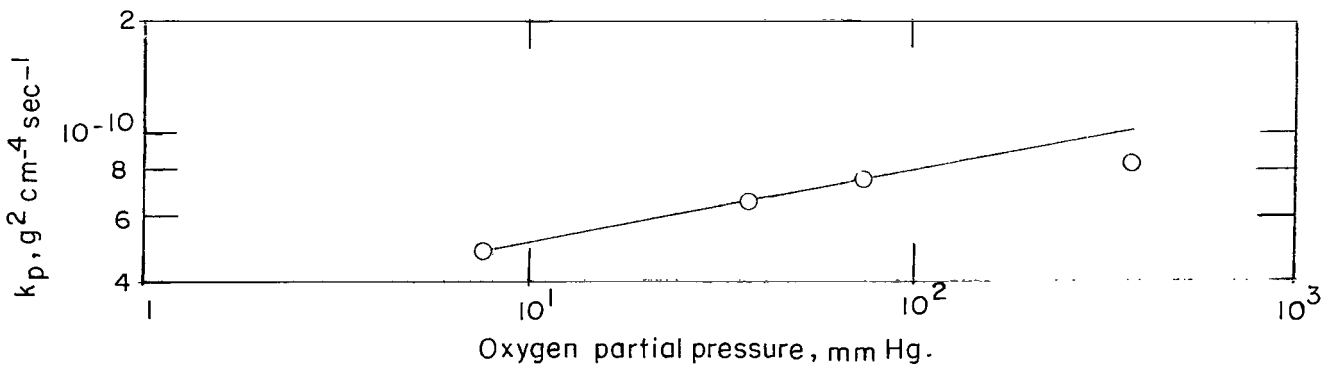

(f) 2000° F, 0.280 standard ft^3/min.

Figure 17.- Continued.

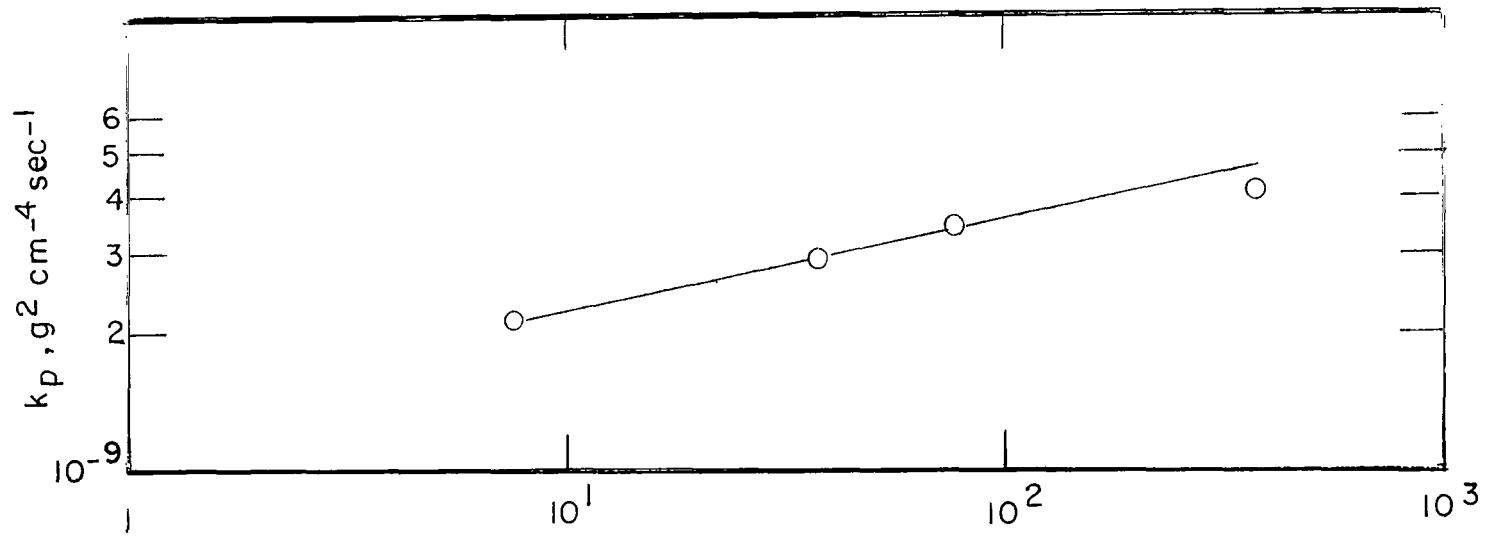

(g) 2250° F, 0.280 standard ft^3/min.

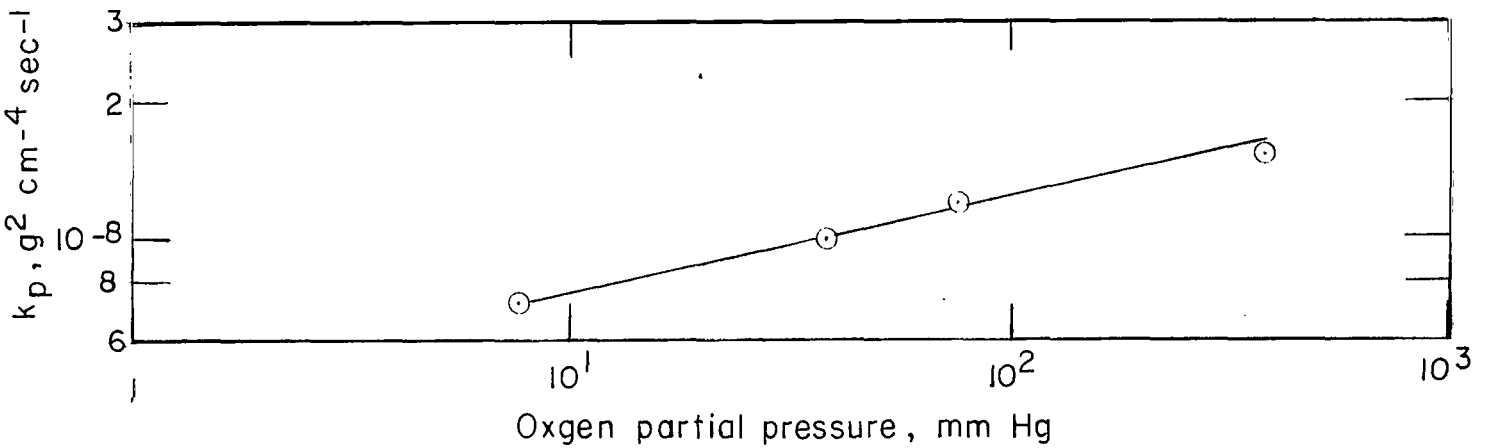

(h) 2500° F, 0.280 standard ft^3/min.

Figure 17.- Concluded.

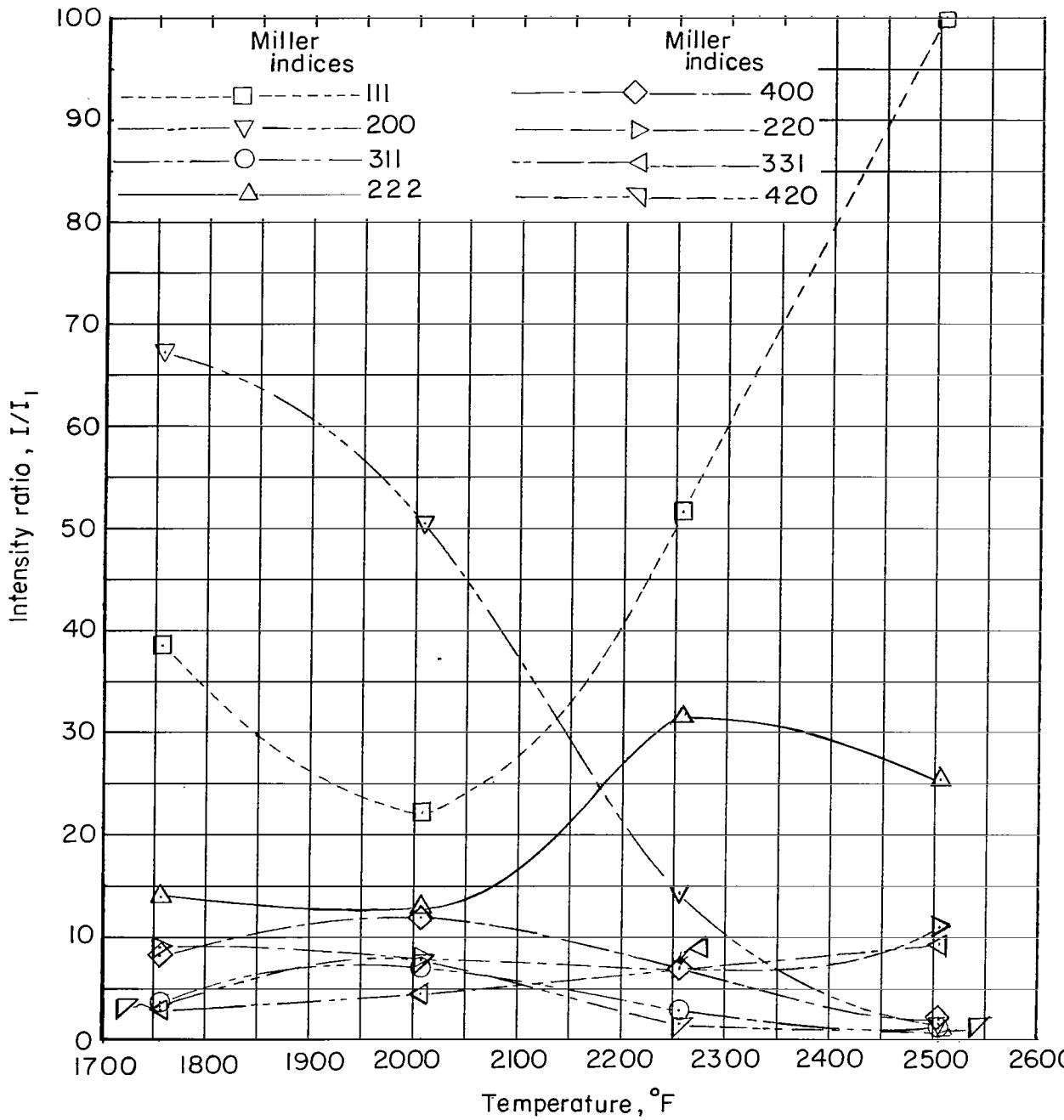

Figure 18.- Variation of peak height (intensity) ratio I/I_1 of NiO lattice planes on outer surface of nickel specimens oxidized at indicated specimen temperatures. 76 mm Hg oxygen partial pressure and 0.130 standard ft^3/min gas flow rate.

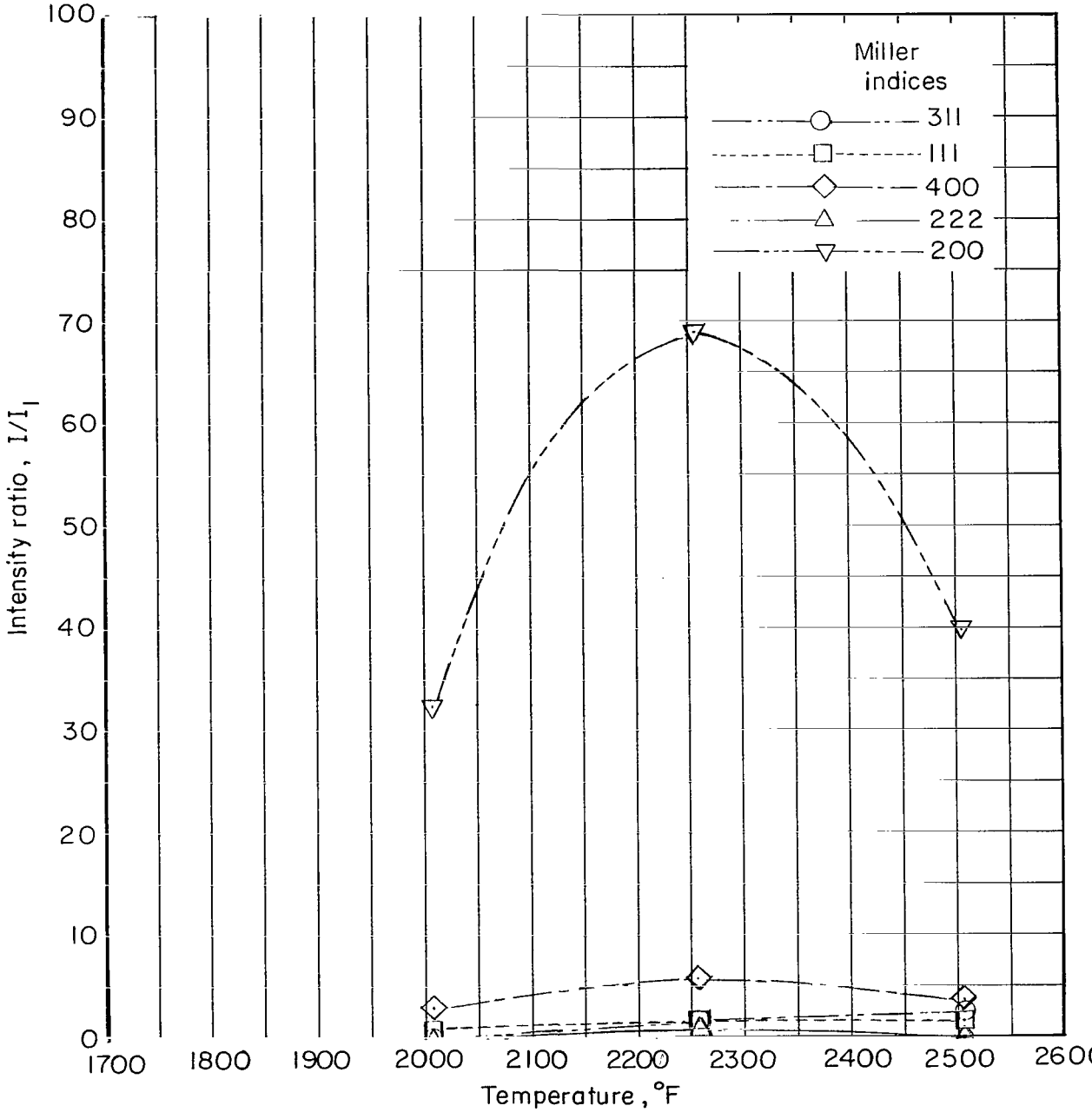

Figure 19.- Variation of peak height (intensity) ratio I/I_1 of NiO lattice planes on subsurface oxide (outer oxide surface removed) of nickel specimens oxidized at indicated specimen temperatures. 76 mm Hg oxygen partial pressure and 0.130 standard ft^3/min gas flow rate.

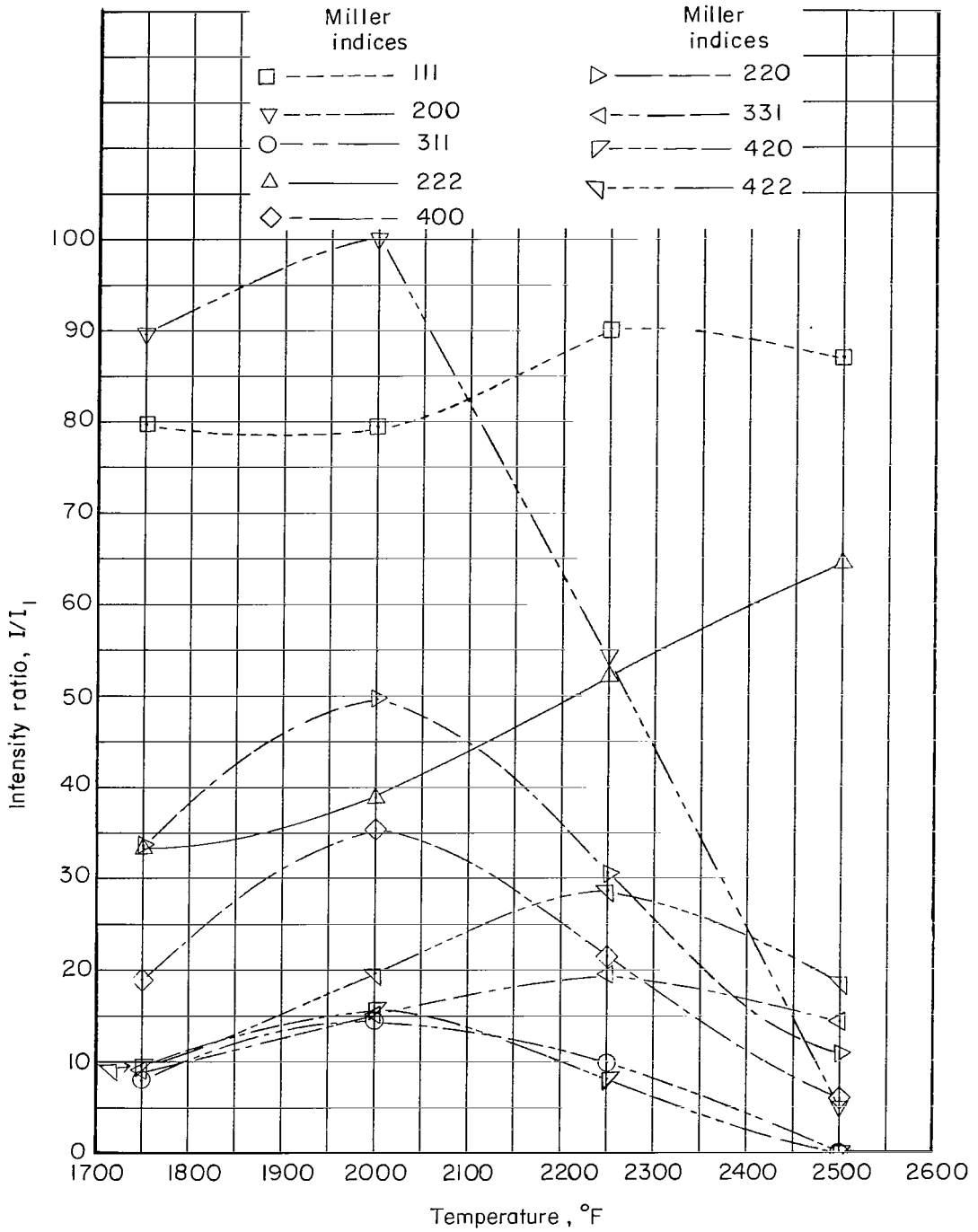

Figure 20.- Variation of peak height (intensity) ratio I/I_1 of NiO lattice planes on outer surface of nickel specimens oxidized at indicated specimen temperatures. 76 mm Hg oxygen partial pressure and 0.280 standard ft^3/min gas flow rate.

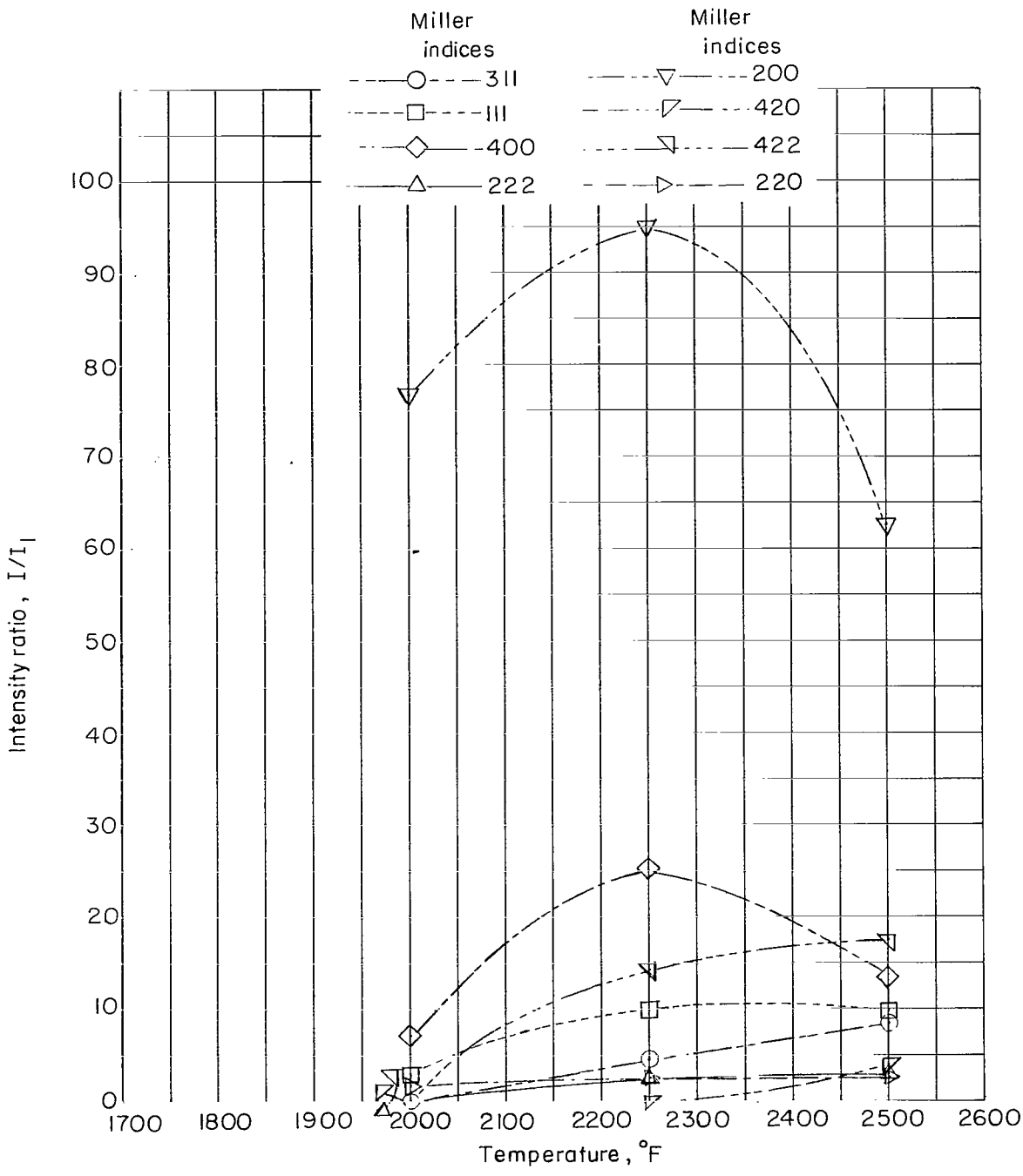

Figure 21.- Variation of peak height (intensity) ratio I/I_1 of NiO lattice planes on subsurface oxide (outer oxide surface removed) of nickel specimens oxidized at indicated specimen temperatures. 76 mm Hg oxygen partial pressure and 0.280 standard ft^3/min gas flow rate.

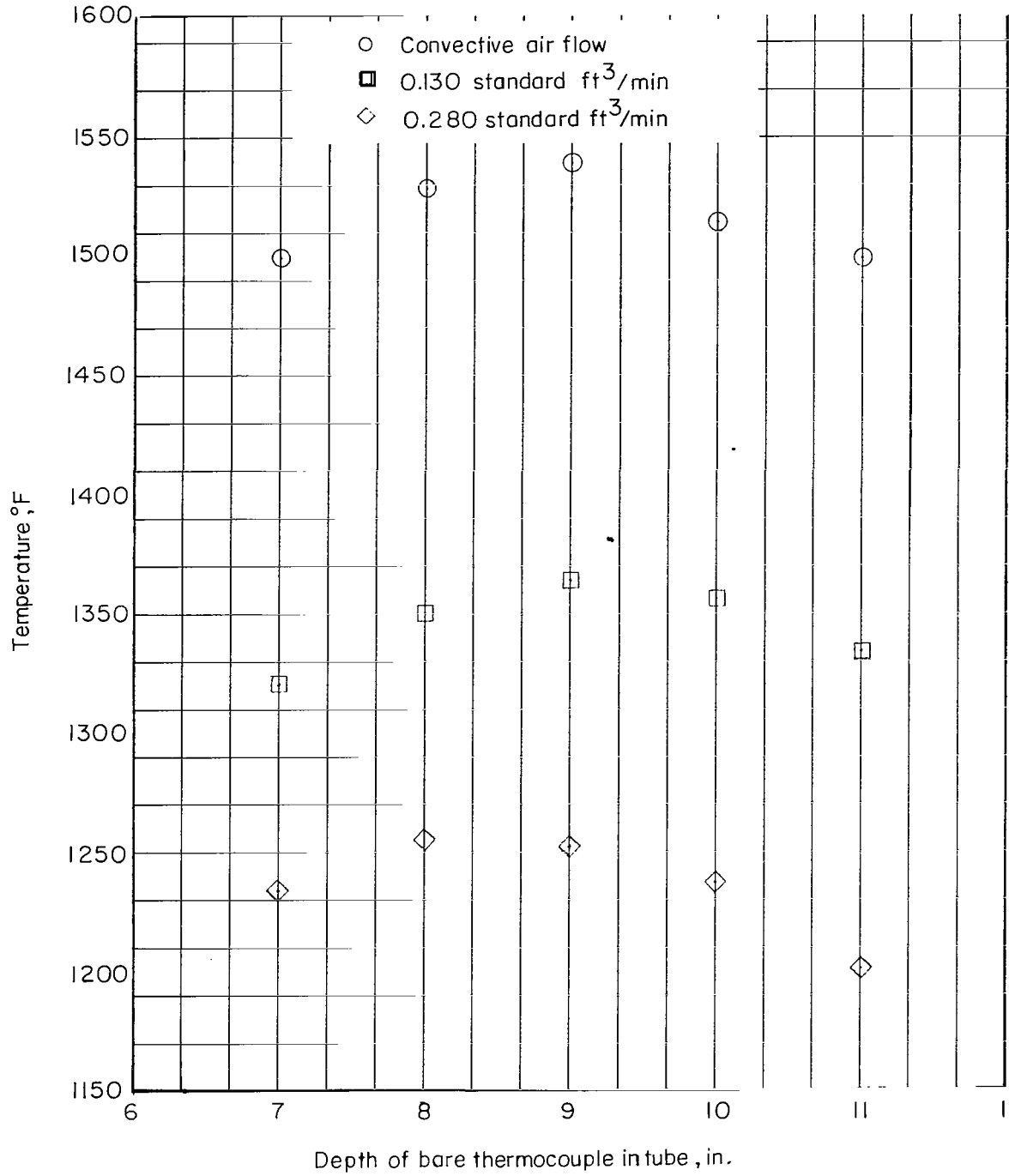

(a) 1500° F nominal furnace temperature.

Figure 22.- Vertical temperature profile of oxidation zone using a bare thermocouple and various air-flow conditions. 1800° F preheater temperature.

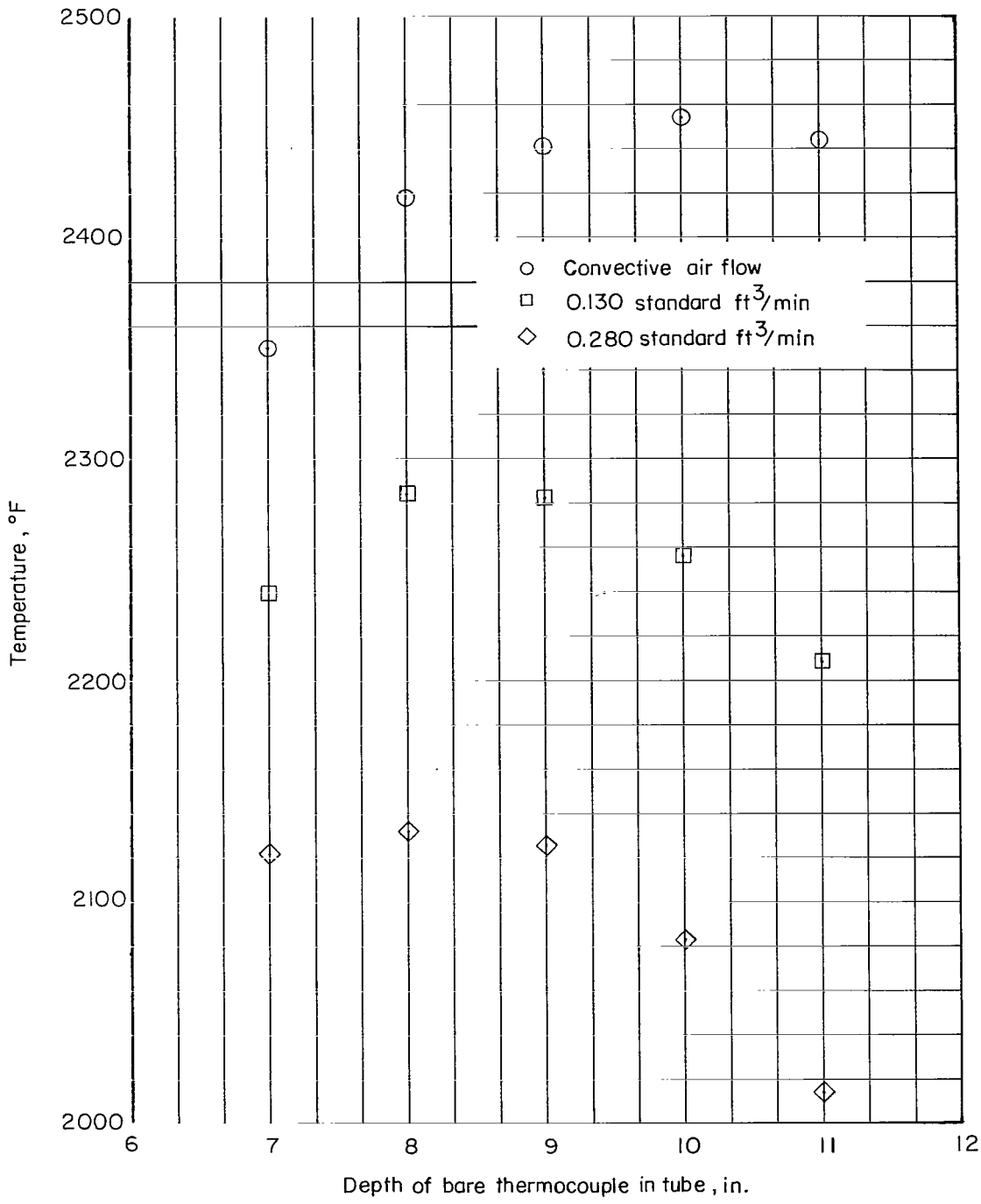

(b) 2500° F nominal furnace temperature.

Figure 22.- Concluded.

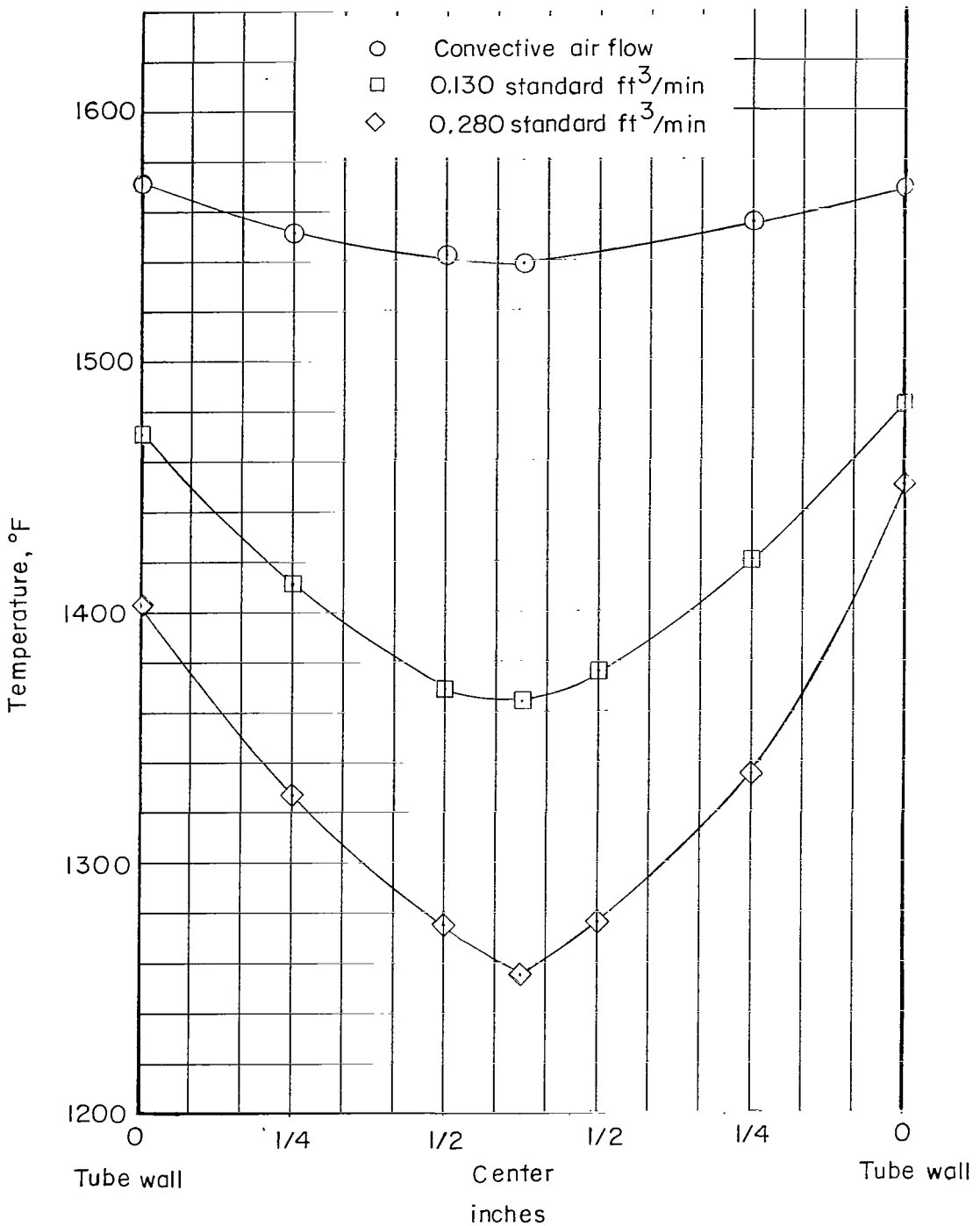

(a) 1500° F nominal furnace temperature.

Figure 23.- Diametric temperature profile of oxidation zone of tube using a bare thermocouple for various air-flow rates. 1800° F preheater temperature.

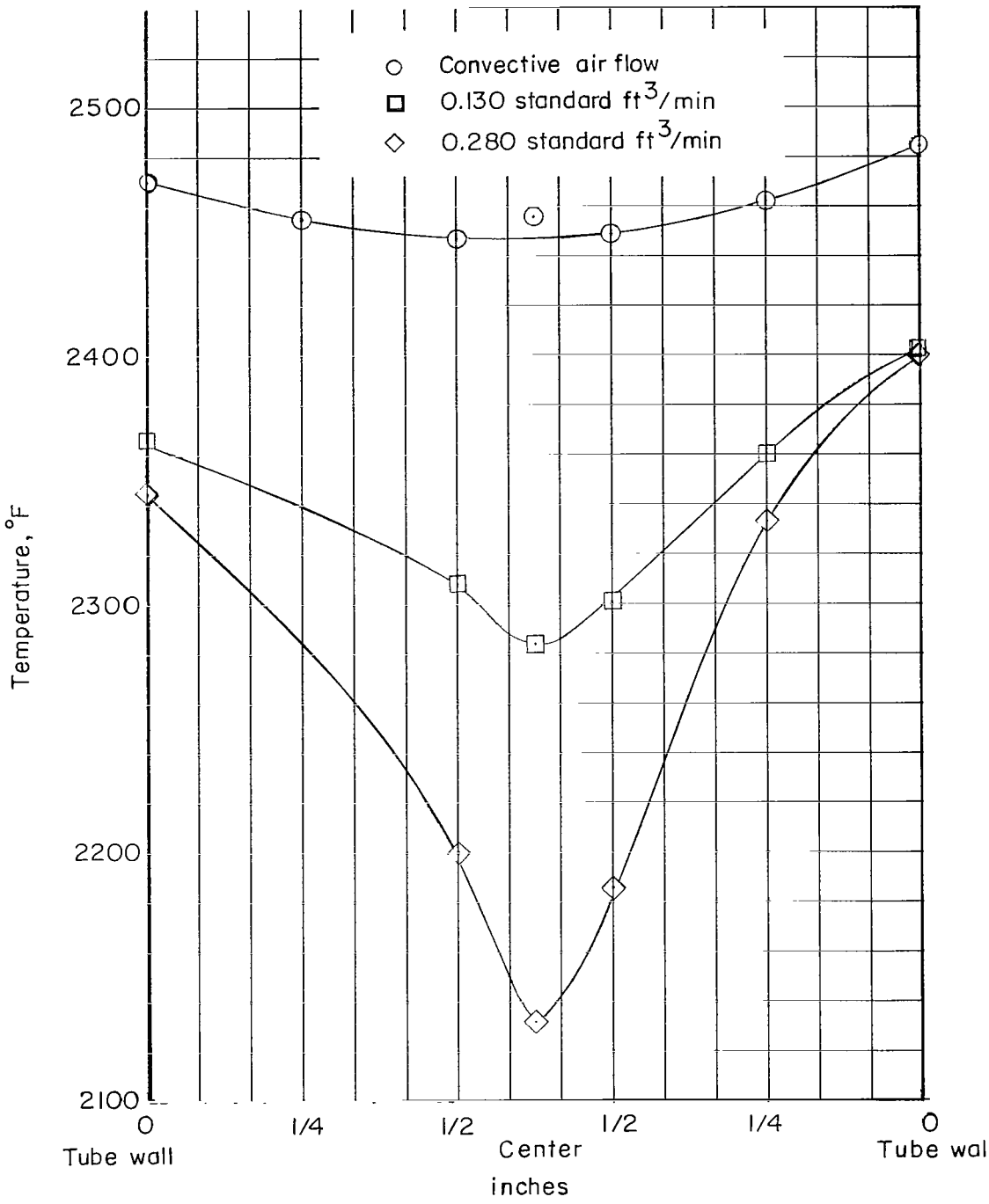

(b) 2500° F nominal furnace temperature.

Figure 23.- Concluded.

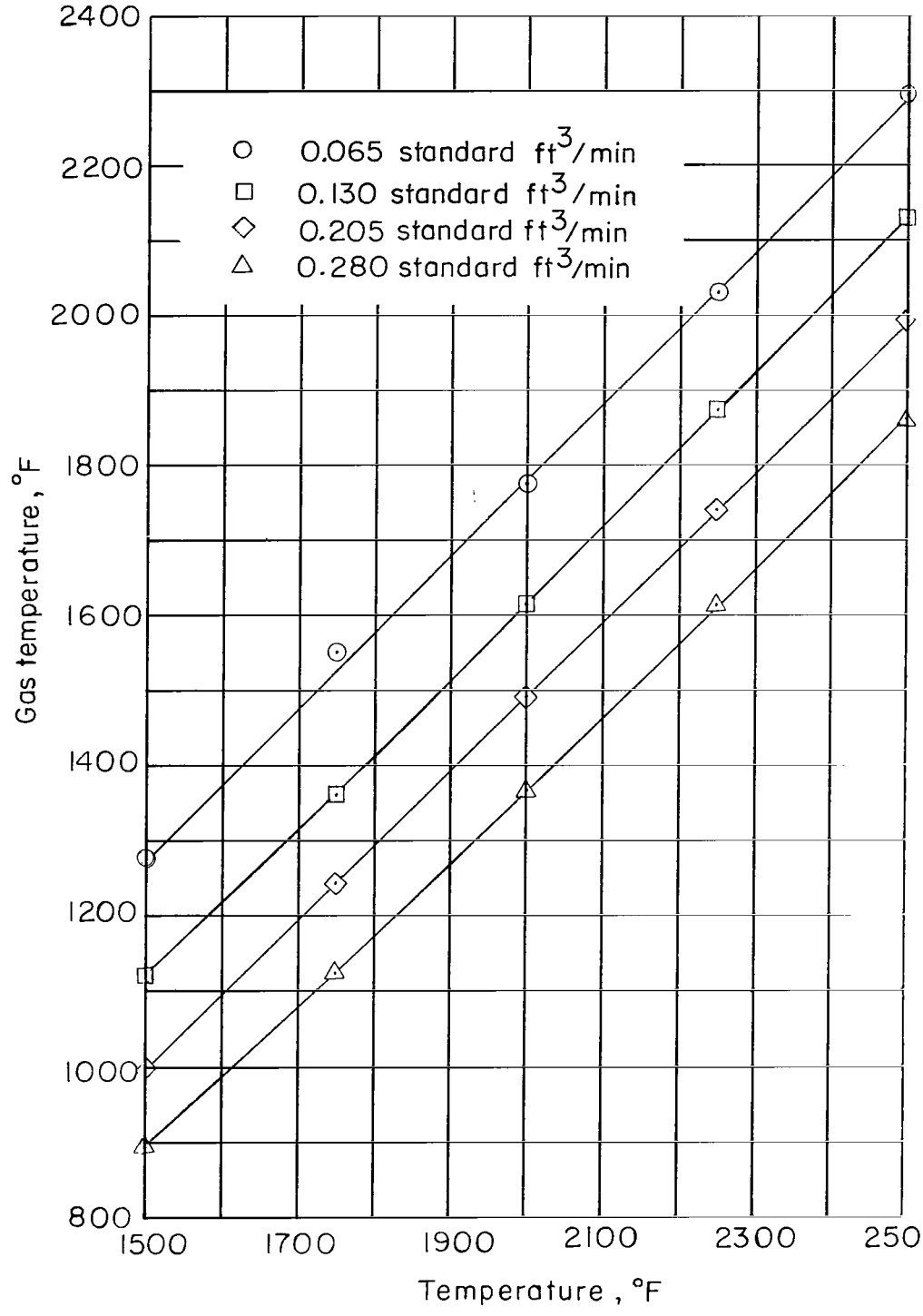

Figure 24.- Variation of gas temperature and specimen temperature at four gas-flow conditions.

2/7/80

"The aeronautical and space activities of the United States shall be conducted so as to contribute . . . to the expansion of human knowledge of phenomena in the atmosphere and space. The Administration shall provide for the widest practicable and appropriate dissemination of information concerning its activities and the results thereof."

—NATIONAL AERONAUTICS AND SPACE ACT OF 1958

NASA SCIENTIFIC AND TECHNICAL PUBLICATIONS

TECHNICAL REPORTS: Scientific and technical information considered important, complete, and a lasting contribution to existing knowledge.

TECHNICAL NOTES: Information less broad in scope but nevertheless of importance as a contribution to existing knowledge.

TECHNICAL MEMORANDUMS: Information receiving limited distribution because of preliminary data, security classification, or other reasons.

CONTRACTOR REPORTS: Technical information generated in connection with a NASA contract or grant and released under NASA auspices.

TECHNICAL TRANSLATIONS: Information published in a foreign language considered to merit NASA distribution in English.

TECHNICAL REPRINTS: Information derived from NASA activities and initially published in the form of journal articles.

SPECIAL PUBLICATIONS: Information derived from or of value to NASA activities but not necessarily reporting the results of individual NASA-programmed scientific efforts. Publications include conference proceedings, monographs, data compilations, handbooks, sourcebooks, and special bibliographies.

Details on the availability of these publications may be obtained from:

SCIENTIFIC AND TECHNICAL INFORMATION DIVISION

NATIONAL AERONAUTICS AND SPACE ADMINISTRATION

Washington, D.C. 20546